

# ON—LINE TOOL—WEAR SENSING AND COMPENSATION DURING TURNING OPERATIONS

*by*

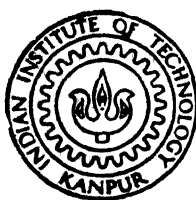
ANUJ SANJANWALA

ME  
1989

M

SAN

ON-L



DEPARTMENT OF MECHANICAL ENGINEERING  
INDIAN INSTITUTE OF TECHNOLOGY, KANPUR  
JANUARY, 1989

# **ON—LINE TOOL—WEAR SENSING AND COMPENSATION DURING TURNING OPERATIONS**

A Thesis Submitted  
In Partial fulfilment of the Requirements  
for the Degree of  
**MASTER OF TECHNOLOGY**

*by*

**ANUJ SANJANWALA**

*to the*

DEPARTMENT OF MECHANICAL ENGINEERING  
INDIAN INSTITUTE OF TECHNOLOGY, KANPUR  
JANUARY, 1989

20 APR 1989  
CENTRAL LIBRARY  
LESTER K. KATZ  

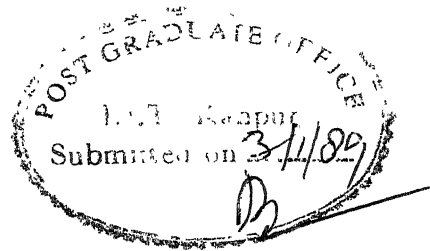
---

Acc. No. A104227

ME-1989-M-SUN-LIN.

72  
621.94  
Sa 58 8

CERTIFICATE



This is to certify that the thesis entitled  
" ON-LINE TOOL-WEAR SENSING AND COMPENSATION DURING  
TURNING OPERATIONS" by Sanjanwala Anuj P., Roll No.  
8620532, is a record of work carried out under our  
supervision and has not been submitted elsewhere for a  
degree.

Dr. V.K. Jain  
Assistant Professor  
Department of Mechanical Engineering  
Indian Institute of Technology  
Kanpur

Dr. S.K. Chaudhury  
Assistant Professor  
Department of Mechanical Engineering  
Indian Institute of Technology  
Kanpur

December, 1988.



ACKNOWLEDGEMENTS

I would like to express my profound gratitude to Dr. S.K. Chaudhury and Dr. V.K. Jain for their precious guidance during the course of this work.

I would like to thank Mr. Jha, Mr. B.P. Bhartiya and Mr. H.P. Sharma for rendering their service available whenever needed.

My sincere thanks are due to my friends Mr. Ngo-Sy-Loc and Mr. K.E. Kapadia for their help and useful suggestions during the course of work.

My thanks to Mr. H.V.C. Srivastava for neat typing and Mr. S.C. Barthwal for tracings.

Finally I am indebted to the previous researchers whose work I had referred to and included Figures from whose papers in the present thesis.

## CONTENTS

	Page
NOMENCLATURE	v
LIST OF FIGURES	vi
LIST OF TABLES	viii
ABSTRACT	ix
 CHAPTER -I INTRODUCTION	
1.1 INTRODUCTION	1
1.2 TOOLWEAR SENSORS	2
1.3 LITERATURE SURVEY	4
1.4 OBJECTIVES AND SCOPE OF THE PRESENT WORK	9
 CHAPTER-II EXPERIMENTAL SET-UP	
2.1 GENERAL LAYOUT	11
2.2 PNEUMATIC SENSOR	14
2.3 SENSITIVITY IMPROVING DEVICE	17
2.4 PILOT-CONTROLLED DIRECTION CONTROL VALVE	18
2.5 ACTUATION MECHANISM	20
2.6 FABRICATION OF THE EXPERIMENTAL SET-UP	20
 CHAPTER-III EXPERIMENTATION	
3.1 OBJECTIVE	22
3.2 PARAMETERS	22
3.3 PREPARATIONS	23
3.4 PROCEDURE	24

CHAPTER-IV	RESULTS, DISCUSSION, CONCLUSIONS AND SCOPE FOR FUTURE WORK	
4.1	RESULTS	27
4.2	DISCUSSION	49
4.3	CONCLUSIONS	50
4.4	SCOPE FOR FUTURE WORK	51
REFERENCES		52
APPENDIX -1		54
APPENDIX -2		55

NOMENCLATURE

$L, d_1$	Distance between nozzle tip and obstruction.
$p$	Backpressure from pneumatic sensor
$P$	Input pressure to the pneumatic sensor
$A$	Constant
$b$	Slope of the straight portion in the pneumatic sensor characteristics
$m$	Area of opening at the nozzle
$C$	Area of the orifice
$D$	Diameter of the nozzle outlet
$d$	Diameter of the orifice
$L_i$	Initial distance between nozzle-tip and obstruction
$L_f$	Final distance between nozzle-tip and obstruction
$E$	Co-efficient of error reduction

LIST OF FIGURES

<u>Figure No.</u>	<u>Title</u>	<u>Page</u>
1.1	Sensor with stylus used by Suzuki and Weinmann.	7
1.2	Diagram of set-up used by EI Gomayel and Bregger.	8
1.3	Set-up of Uehara and Shiraishi	9
1.4	Set-up of Park, Eman and Wu.	9
2.1	Diagram showing effect of toolwear on dimensional accuracy.	11
2.2	Schematic diagram of the experimental set-up.	12
2.3	Nozzle-orifice assembly.	14
2.4	Characteristics of the pneumatic sensor.	17
2.5	Fixture for mounting nozzle on the centre lathe.	17
2.6	Sensitivity improving device.	17
2.7	Pilot-controlled direction control valve.	19
2.8	Actuator mechanism.	20
4.1	Graph showing results of experiment -1	28
4.2	Graph showing results of experiment -2	29

<u>Figure No.</u>	<u>Title</u>	<u>Page</u>
4.3	Graph showing results of experiment -3	30
4.4	Graph showing results of experiment -4	31
4.5	Graph showing results of experiment -5	32
4.6	Graph showing results of experiment -6	33
4.7	Graph showing results of experiment -7	34
4.8	Graph showing results of experiment -8	35
4.9	Graph showing results of experiment -9	36
4.10	Graph showing results of experiment -10	37
4.11	Graph showing results of experiment -11	38
4.12	Graph showing results of experiment -12	39
4.13	Graph showing results of experiment -13	40
4.14	Graph showing results of experiment -14	41
4.15	Graph showing results of experiment -15	42
4.16	Graph showing results of experiment - 16	43
4.17	Tool 1,2,3 and 4	45
4.18	Tool 5,6,7 and 8	46
4.19	Tool 9,10,11 and 12	47
4.20	Tool 13,14,15 and 16	48

LIST OF TABLES

<u>Table No.</u>	<u>Title</u>	<u>Page</u>
1	Results of experiment -1	28
2	Results of experiment -2	29
3	Results of experiment -3	30
4	Results of experiment -4	31
5	Results of experiment -5	32
6	Results of experiment -6	33
7	Results of experiment -7	34
8	Results of experiment -8	35
9	Results of experiment -9	36
10	Results of experiment -10	37
11	Results of experiment -11	38
12	Results of experiment -12	39
13	Results of experiment -13	40
14	Results of experiment -14	41
15	Results of experiment -15	42
16	Results of experiment -16	43
17	Co-efficients of error reduction for same feed but different speeds.	44

### ABSTRACT

Toolwear results in uneconomical machining conditions and dimensional inaccuracy. In past much attention was focused on avoiding the uneconomical machining conditions by timely replacement of the tool. Not many efforts have been made to avoid dimensional inaccuracies during a single long cut.

In turning operations the diameter of the workpiece increases along the length of cut due to the flank toolwear. In this thesis an attempt has been made to design and fabricate a system which can be mounted on a centre lathe and improve dimensional stability by on-line toolwear sensing and compensation. The proposed system was realized by a pneumatic sensor to sense the on-line toolwear, a device to improve sensitivity, a pilot-controlled direction control valve to amplify the signal from the pneumatic sensor and an actuation mechanism to move the tool for compensating dimensional inaccuracies.

The proposed system is tested for various cutting conditions. The improvement in the dimensional stability is shown by taking a cut with pneumatic-sensor feedback and then repeating the cut with identical cutting conditions but without feedback. The error was measured and compared.

The results show, that using the developed system error was reduced considerably and restricted to 0.042 mm at the highest.



## CHAPTER I

### INTRODUCTION

#### 1.1 INTRODUCTION :

The primary method of imparting form and dimension to a workpiece is the removal of material by the use of edged cutting tools. While the extra material is being removed from the workpiece, the tool also loses some material in the process. Cutting tools having sufficient strength against failure by brittle fracture or loss of form stability through rise of interface temperature, still continue to fail by a process known as wear which is loss of cutting tool material through gradual interaction between the work and the tool material. Tool wear may take place either at the principal flank surface (i.e., flank face) or at the top face of the cutting tool (i.e., rake face of the tool) for roughing and semi-roughing cuts. Wear may also occur at the auxiliary flank surface resulting in grooving wear during fine machining or machining of high strength materials.

The causes for such wear process include.

- i) Mechanical interaction (Abrasion or adhesion and transfer type)
- ii) Thermochemical interaction (Diffusion or chemical reaction)

The tool wear may result in one or more of the following events :

- i) Increase in cutting force
- ii) Loss of accuracy
- iii) Deterioration of surface finish
- iv) Increase in cutting temperature
- v) Increase in vibrations.

The aforementioned consequences of the toolwear indicate that on-line monitoring of the toolwear is bound to result in reduced cost of machining and improvement in the quality of the product. Hence, efforts were made to develop Adaptive Control Optimization (ACO) Systems which account for the toolwear and also control the system performance.

One of the most complex problems arising in the development of Adaptive Control Optimization Systems is a correct choice of the wear sensor that should have high accuracy, reliability and be economical at the same time. Some of the details of the sensors are discussed below.

## 1.2 TOOLWEAR SENSORS :

### 1.2.1 Requirements :

Some of the qualities that the successful toolwear sensor must have are

- i) It must give a clear and reliable signal.
- ii) It must be robust so as to be able to operate under the shopfloor conditions.
- iii) It must have fast response to toolwear.
- iv) It should be as flexible as possible so as to be used with a variety of machining processes.
- v) It should not interfere with the machining process.
- vi) It should be cheap and safe to use under shopfloor conditions.
- vii) It must provide signal that can be linked to the machine control system.

#### 1.2.2 Classification :

Toolwear sensors are categorised into direct or indirect type. The direct methods are those that utilize effects caused directly by toolwear. The indirect methods measure parameters that change to some degree with toolwear.

Some direct and indirect methods are listed below :

##### Direct Methods.

- i) Radioactivity method
- ii) Pneumatic method
- iii) Electrical resistance method
- iv) Optical method

### Indirect Methods

- i) Measuring cutting forces
- ii) Measuring workpiece dimensions
- iii) Measuring surface finish
- iv) Measuring cutting temperature
- v) Sensing Vibrations
- vi) Analysing acoustic signal

### 1.3 LITERATURE SURVEY :

This section reviews the available literature on toolwear sensing and compensation.

Merchant, Ernst and Krabacher<sup>(1)</sup> devised an abbreviated method of measuring cutting tool-life using radioactive isotopes as tracers to measure the instantaneous rate of toolwear. The method consisted of machining with a tool which had been rendered radioactive by neutron irradiation in a nuclear reactor, collecting the resulting chips and measuring their radioactivity due to particles abraded from tool during a few seconds of cutting. Although the toolwear was measured off-line here the on-line measurement was later carried out by other researchers<sup>(2),(3)</sup> based on the same principle.

Cook, Subramaniam and Merchant<sup>(2)</sup> developed a tool wear sensor which used micro-isotope. An exceedingly small (less than  $10^{-8}$  curies) amount of radioactive material was implanted in the flank face at a known distance apart from the cutting edge. When flankwear progressed beyond this point the active material was removed. At the end of each cutting cycle, a sensor determined in a few seconds whether or not wear had progressed that far.

Arsovski<sup>(3)</sup> tested a sensor based on the measurement of the radioactivity of the activated cutting elements of the tool during cutting. The radioactivity of the tool was strongly correlated with the size of the wearland at the cutting elements. The radioactivity of the tool was continuously measured during cutting and the toolwear could be determined with the accuracy of 0.002 mm.

Wilkinson<sup>(4)</sup> used the concept of the constriction resistance which is a function of the area of contact between the cutting tool and the workpiece.

Staferle and Bellmann<sup>(5)</sup> developed a pneumatic system for toolwear sensing. The concept of back pressure increase with reduction in the distance between flapper and a nozzle was used. The workpiece acted as a flapper.

Weller, Schrier and Weichbrodt<sup>(6)</sup> developed an electromechanical system which utilized sonic signals to detect the degree of cutting edge wear in metal-working tools and automatically triggered a cutting edge change. A packaged electronic unit was developed to readout sonic vibrations from an instrumented machinetool-workpiece-cuttingtool system to determine the degree of cutting edge wear during a turning operation. At a predetermined comparative sonic ratio, the electronic unit commanded stoppage of the machinetool feed, retraction of the tool and automatic index of the cemented carbide insert to the next undamaged cutting edge. The later function was performed by a prototype mechanical device.

Emel and Kannatey Asibu Sr.<sup>(7)</sup> developed a technique for detection of toolwear, toolfracture or chip disturbance events using the spectra of acoustic signals generated by these sources. In addition, a methodology for determining the feature dimensionality, the selection of best features and the minimum training sample size was presented. The concept of classification error minimization and manufacturing cost minimization had been applied to design classifiers using a hierarchical decision strategy to improve the performance of tool failure sensing.

Colwell<sup>(8)</sup> developed a system that tracked tool deterioration using a computer. The technique basically consist of measuring the ratio of the forces acting on the flank of the tool and rakeface of the tool.

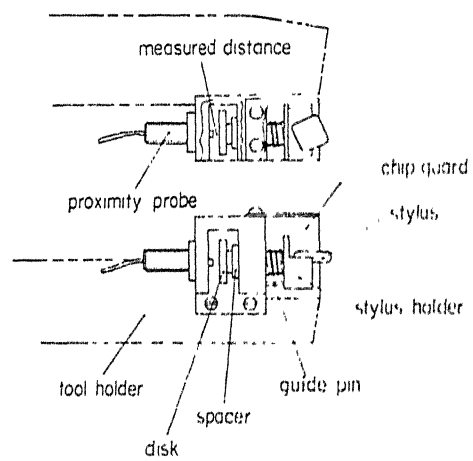


Fig. 1.1: Sensor with stylus used by Suzuki and Weinmann.

Uehara<sup>(9)</sup> proposed a method of automatic monitoring of the wear of the cutting tools in NC turning. The method was based on an experimental fact that the pattern of curve which shows the relationship between the cutting force (feed force) and the feed per revolution is strongly influenced by the toolwear. A special NC program was inserted at the beginning of NC tape per workpiece instead of conventional roughing program with which material is removed, and the feed force was measured corresponding to the action of the special NC program. Then, the automatically obtained feedforce oscillogram shows the feed forcefeed/revolution diagram because the special NC program is made to increase the feed from zero to a predetermined value in small steps at every five revolutions.

Suzuki and Weinmann<sup>(10)</sup> devised an online toolwear sensor by measuring the change in distance between tool holder and workpiece using a stylus which is mounted on a toolholder. The stylus movement is sensed by a displacement transducer. The toolwear was monitored using a digital processing oscilloscope. The sensor is shown in Figure 1.1 .

El Gomayel and Bregger<sup>(11)</sup> developed a toolwear sensor that used indirect method of monitoring the change in the workpiece diameter during turning operation. The change in the diameter was sensed by electromagnetic sensors which



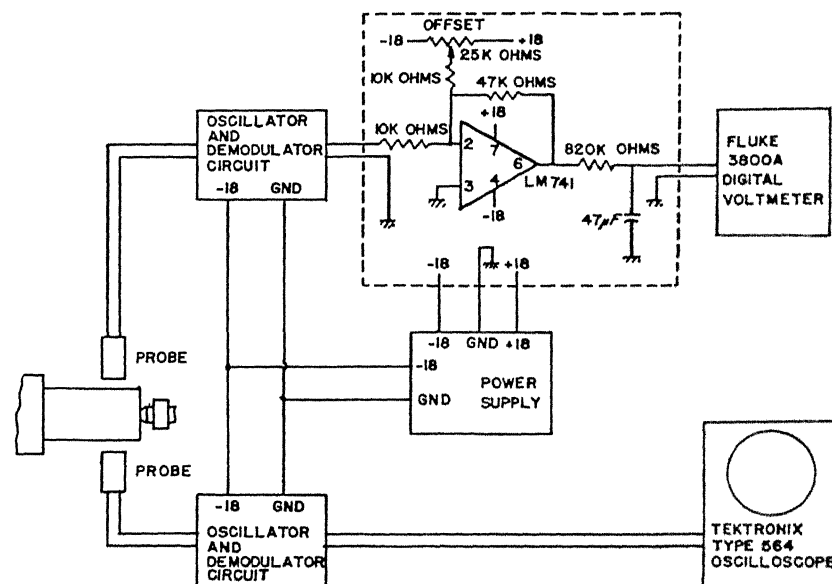


Fig. 1.2 : Diagram of set-up used by AT Gomayel and Bregger.

gave voltage output directly related to the gap between the sensor and the workpiece. Two sensors were operated in a differential mode to compensate for deflections and vibrations. The set-up-blockdiagram is shown in Figure 1.2.

Maeda, Uchida and Yamamoto<sup>(12)</sup> developed a measuring system in which an overall geometric feature of the tool tip in microscopic view was described as a 2-dimensional (2D) digital picture, from which every ordinary machining parameters (crater wear depth, flank land width, etc.) can be obtained easily with the aid of digital picture processing technique.

National Bureau of Standards<sup>(5)</sup> of United states developed a sensor that recognized drillwear and predicted drill breakage by applying time domain analysis to signals from an accelerometer attached to the workpiece.

The research division of Bendix<sup>(5)</sup> of United States investigated a system that monitored infrared radiation from the cutting edge as an indication of temperature.

In the above mentioned research works the idea was to measure the toolwear and replace the worn tool by an undamaged one at a proper time, so as to avoid uneconomical cutting conditions or to advance the tool before taking a fresh cut in order to compensate for the tool off-set. No consideration was given to the inaccuracies arising in a single

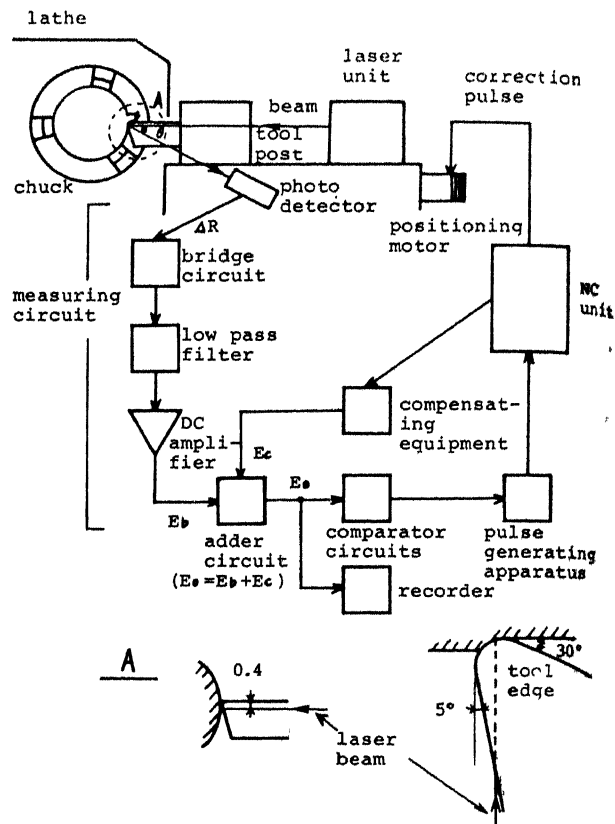


Fig. 1.3 : Set-up of Uehara and Shiraishi.

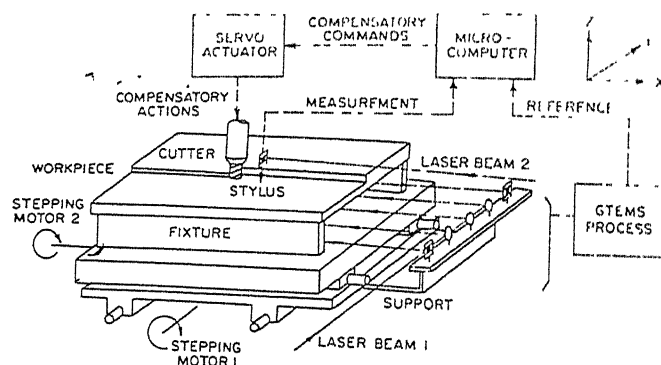


Fig 1 Overall configuration of the proposed set-up

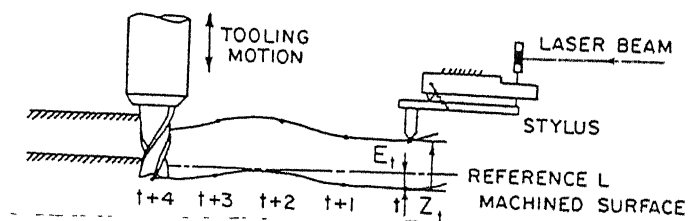


Fig. 1.4 : Set-up of Park, Eman and Wu.

long cut due to wear of the tool. The attempt in this direction was made by Shiraishi and Uehara in 1979.

Shiraishi and Uehara<sup>(13)</sup> developed a non-contact measuring apparatus of workpiece dimensions. They used this apparatus for in-process control on NC lathe. The apparatus proposed was realized by the use of a laser unit, photoconductive cells and optical systems. The finished size of a workpiece was continuously monitored by the laser spot and the toolpost was automatically moved in the direction to reduce the error. The schematic diagram of the system is shown in Figure 1.3.

C.W. Park, K.F. Eman and S.M. Wu<sup>(14)</sup> developed a laser based system for in-process measurement of flatness errors and compensation in milling operations. The basic idea was to measure the workpiece error in-process, find stochastic model, forecast the future values of the error and compensate the milling cutter position vertically through a hydraulic drive system. The schematic arrangement of the set-up is shown in figure 1.4.

#### 1.4 OBJECTIVES AND SCOPE OF THE PRESENT WORK :

The present work is aimed in the field of online dimensional control of workpiece in turning operation on a centre lathe. In the past much attention has been paid to the online toolwear sensing in order to avoid uneconomical

machining conditions that arise due to excessive toolwear. Apart from few exceptions<sup>(13)(14)</sup> attention was not paid to the inaccuracies arising due to toolwear while machining considerably long workpieces. In turning operations, the tool off-set was compensated after the cut was over and not while the operations was on. The present work involves on-line sensing and compensation of toolwear in turning operation on a centre lathe so as to avoid uneconomical machining conditions and achieve on-line dimensional control. The objectives of the present work can be subdivided in the following subheadings :

- i) Design and fabrication of a sensing device to sense toolwear during machining of a workpiece.
- ii) Selection of an actuator to position the toolpost according to the toolwear.
- iii) Design and fabrication of a feedback control system components that connect the sensing and compensating components.
- iv) Assembly and testing of the designed and fabricated system.

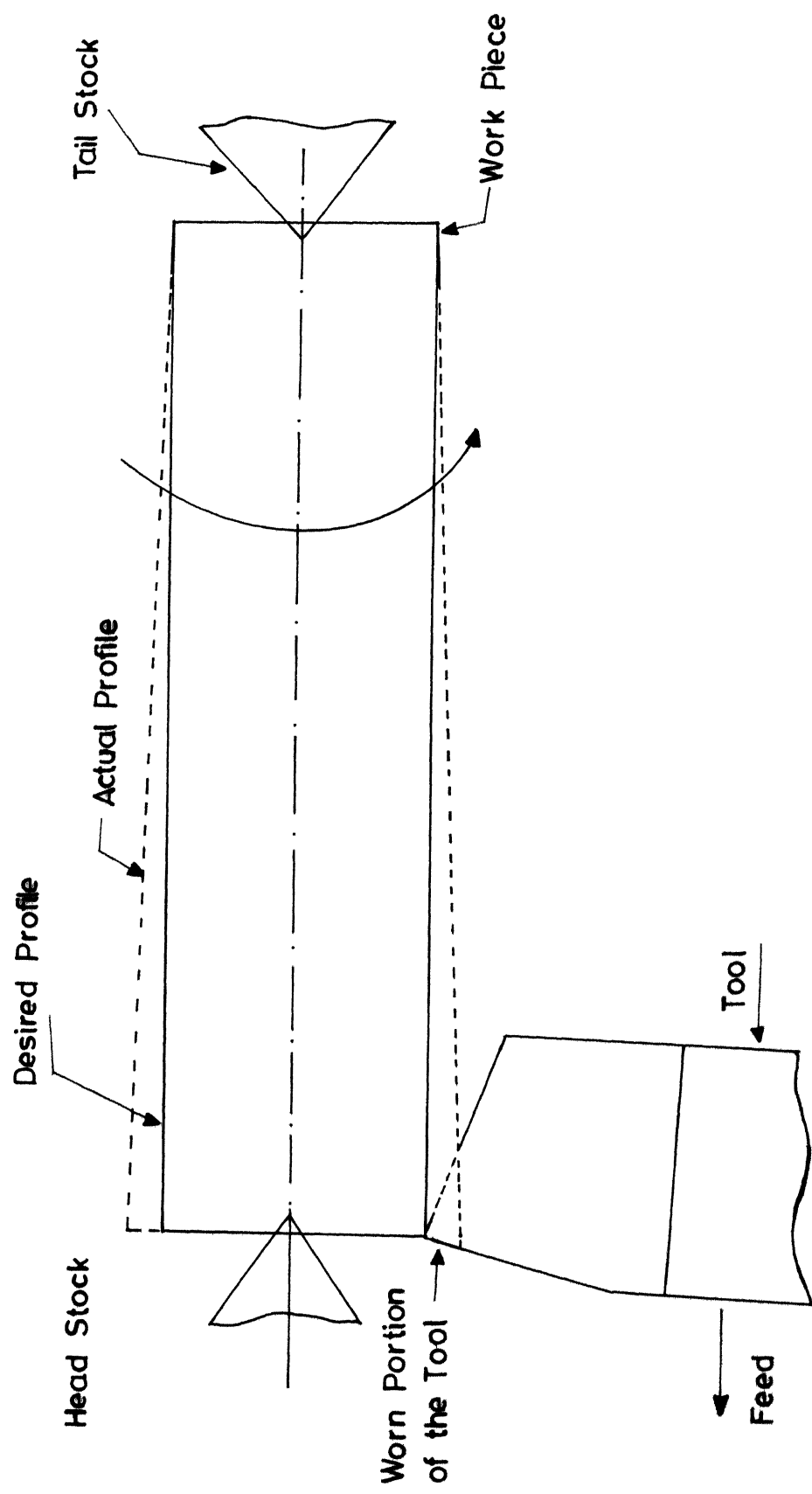


Fig.2.1 Diagram Showing Effect of Tool-wear on Dimensional Accuracy .

## CHAPTER -II

### EXPERIMENTAL SET-UP

#### 2.1 GENERAL LAYOUT :

It was mentioned in the previous chapter that the dimensional stability of the workpiece is adversely affected by the toolwear in any machining process. Figure 2.1 schematically shows how the diameter of the workpiece being turned on a centre lathe would increase along the length due to the radial toolwear. The radial toolwear comprises of the nose wear and the component of the flank wear in the radial direction. Both of these combined can affect the dimensional stability considerably. In order to maintain the dimensional stability the tool must be moved towards the workpiece axis by the same amount as the magnitude of the radial toolwear.

The fact that the diameter of the workpiece would increase along the length in proportion to the radial toolwear, can be used to sense the toolwear. However a good sensor is required to sense the increase in the dimension of the workpiece while it is being machined. In past the pneumatic on-line sensors have been used to measure the change in the workpiece diameter. In present work also the pneumatic sensor was chosen to sense the increment in the diameter along the length during the turning operations. A nozzle-orifice assembly acts as a sensor.

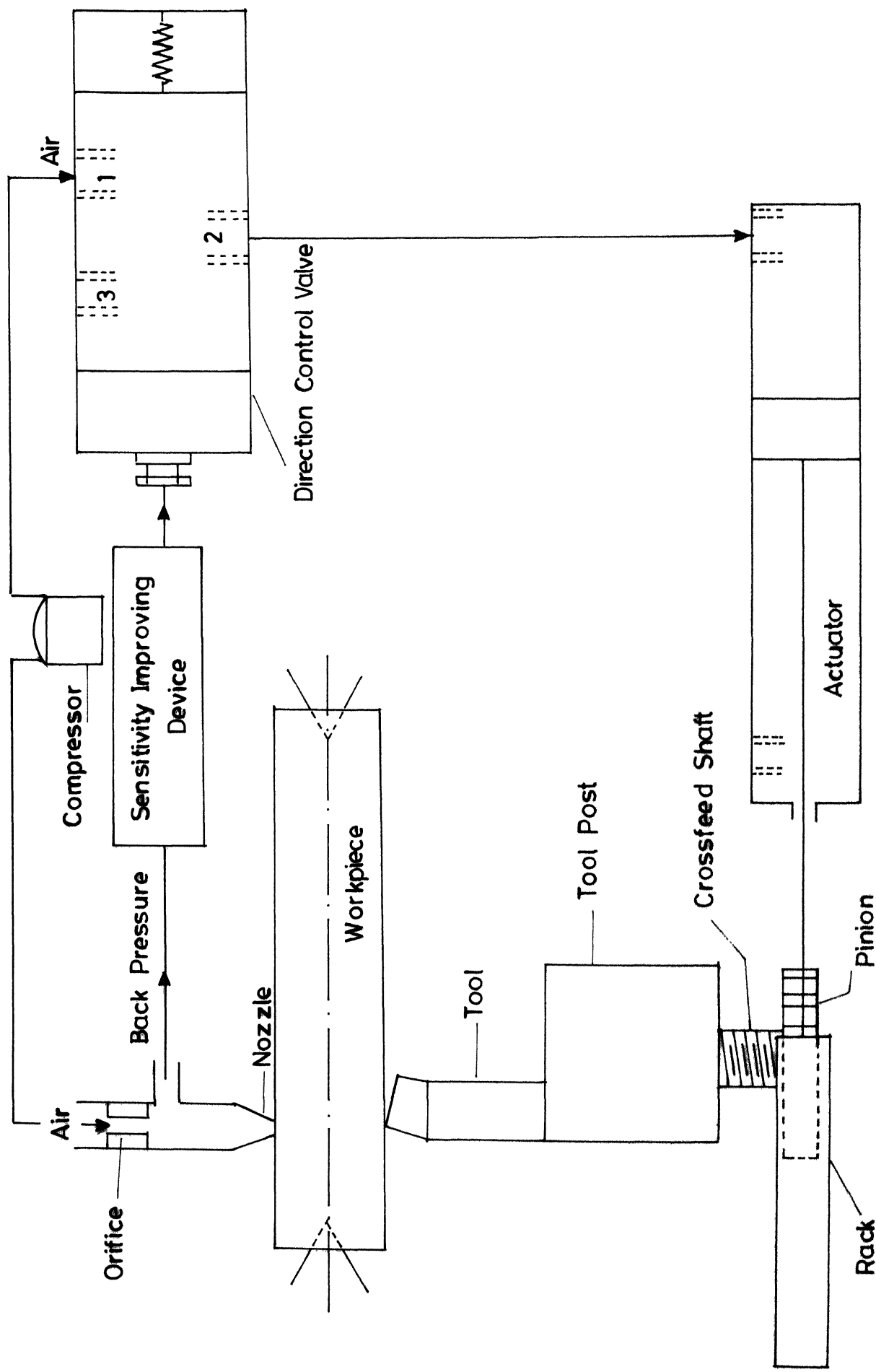


Fig . 2.2 Schematic Diagram of the Experimental Set-Up .



The signal provided by the pneumatic sensor is also pneumatic. An actuation mechanism is necessary to convert this pneumatic signal into the mechanical displacement and move the tool towards the workpiece axis. A gear is mounted on the cross feed screw of the centre lathe and an actuator is connected to this gear by a rack to accomplish this.

The pneumatic signal given by the pneumatic sensor is not powerful enough to actuate the tool. Some amplification is required in order to create a signal powerful enough to actuate the tool. A pilot-controlled direction control valve is used to amplify the signal generated by the pneumatic sensor.

A sensitivity improving device was used to improve the overall sensitivity of the system.

Figure 2.2 schematically shows the general layout of the experimental set-up. A compressor is used as a source of the compressed air. The compressor surge tank has two openings. The one is connected to the pneumatic sensor by a control valve and a conduit and the other one is connected to the manport of the pilot controlled direction control valve. The air coming to the pneumatic sensor first passes through an orifice and then through a nozzle. The pressure between orifice and nozzle is called backpressure and it depends on the distance between the nozzle

and the workpiece which decreases with the increase in the diameter of the workpiece along the length. In other words the backpressure increases with the wear of the tool. This backpressure is taken to the sensitivity improving device. This device does not let the air through unless and until backpressure reaches a predetermined level. From sensitivity improving device the air goes to the pilot port of the pilot-controlled direction control valve. The valve remains closed unless and until air at certain pressure enters the pilot port. A manport of this valve is connected to the compressor and when the valve opens air at full compressor pressure passes through the valve and enters the actuator. The pressure acting on actuator piston is sufficient to displace it against the radial cutting force and the frictional forces. Hence the toolwear is compensated and the desired diameter of the workpiece being turned is restored.

Summarizing, as the tool wears during turning the diameter of the workpiece being turned increases. This results in the increase in the backpressure from the pneumatic sensor. This increased backpressure opens the pilot-controlled direction control valve. This allows the compressor to be connected to the actuator and the tool moves forward. As the tool moves forward the desired diameter of the workpiece being

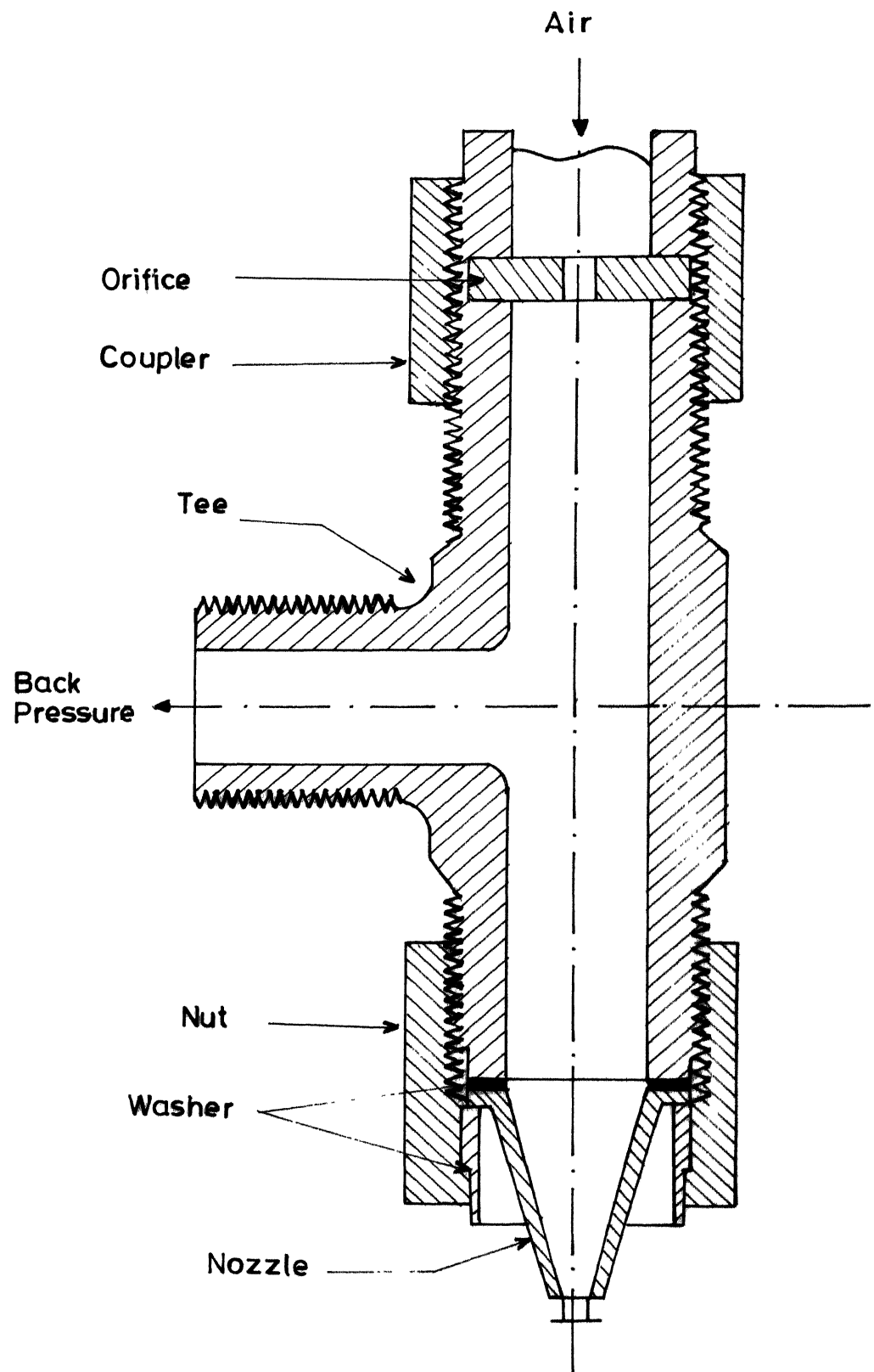


Fig.2.3 Nozzle Orifice Assembly .

machined is restored and the backpressure decreases. The direction control valve closes with decrease in the backpressure and compressor is disconnected from the actuator and hence the actuation stops.

## 2.2 PNEUMATIC SENSOR :

A pneumatic sensor was designed and fabricated in the form of a nozzle-orifice assembly which is shown in figure 2.3. The diameters of nozzle and orifice play important role in deciding the sensitivity of the sensor and hence were to be carefully chosen. The diameter of the nozzle and orifice should be chosen considering the difficulties of manufacturing.

In pilot-controlled direction control valve there is a considerable amount of friction between the sliding surfaces. The valve was found to open at  $0.6 \text{ kg/cm}^2$  and close at  $0.2 \text{ kg/cm}^2$ . The highest input pressure that can be maintained constant over a period of time was found to be  $0.9 \text{ kg/cm}^2$  with available air-compressor. Taking all these facts into account the diameter of the orifice was selected to be 2.0 mm and the diameter of the nozzle out-let was selected to be 2.5 mm. Considering the fact that the sensitivity improving device can be adjusted so that it would open at  $0.55 \text{ kg/cm}^2$  the sensitivity of the experimental set-up can be calculated as follows.

Equation of the linear portion of any nozzle-orifice characteristics is

$$\frac{p}{P} = A - b (m/c) \quad \dots (2.1) \quad (15)$$

where

$p$  = Backpressure

$P$  = Input pressure

$A$  = 1.1 in all the cases

$b$  = Slope of the straight portion

$m$  = Area of opening at the nozzle

$c$  = Area of the orifice

$$m = \pi DL \quad \dots (2.2)$$

where  $D$  = Diameter of the nozzle outlet

$L$  = Distance between nozzle-tip and the obstruction

The nozzle would have better characteristics if the obstruction was perfectly flat. But in the present work the workpiece surface acts as an obstruction and it is cylindrical. However for calculation purpose it is assumed to be flat in equation 2.2.

$$c = \pi d^2/4 \quad \dots (2.3)$$

where  $d$  = Diameter of the orifice

Substituting 2.2 and 2.3 in 2.1 we get,

$$\frac{p}{P} = A - b \left( \frac{\pi DL}{\pi d^2/4} \right) \quad \dots (2.4)$$

Initially

$$p = 0.55 \text{ kg/cm}^2$$

$$P = 0.9 \text{ kg/cm}^2$$

Corresponding  $L = L_i$  is calculated as follows  
from 2.4

$$\frac{p}{P} = A - b \left( \frac{4DL}{d^2} \right)$$

$$\therefore b \left( \frac{4DL}{d^2} \right) = A - \frac{p}{P}$$

$$\therefore L = \left( A - \frac{p}{P} \right) \frac{d^2}{4bD} \quad \dots (2.5)$$

(15) Selecting value of  $b$  to be 1.5 from the existing  
data and substituting other values

We get

$$L_i = 0.133 \text{ mm.}$$

Now for  $L$  corresponding to valve-opening  $L_f$  the  
value of  $p$  is taken as  $0.6 \text{ kg/cm}^2$  and substituted in  
equation 2.5.

$$L_f = 0.116 \text{ mm.}$$

$$\begin{aligned} \text{Theoretical sensitivity} &= L_i - L_f \\ &= (0.133 - 0.116) \text{ mm} \\ &= 0.017 \text{ mm} \end{aligned}$$

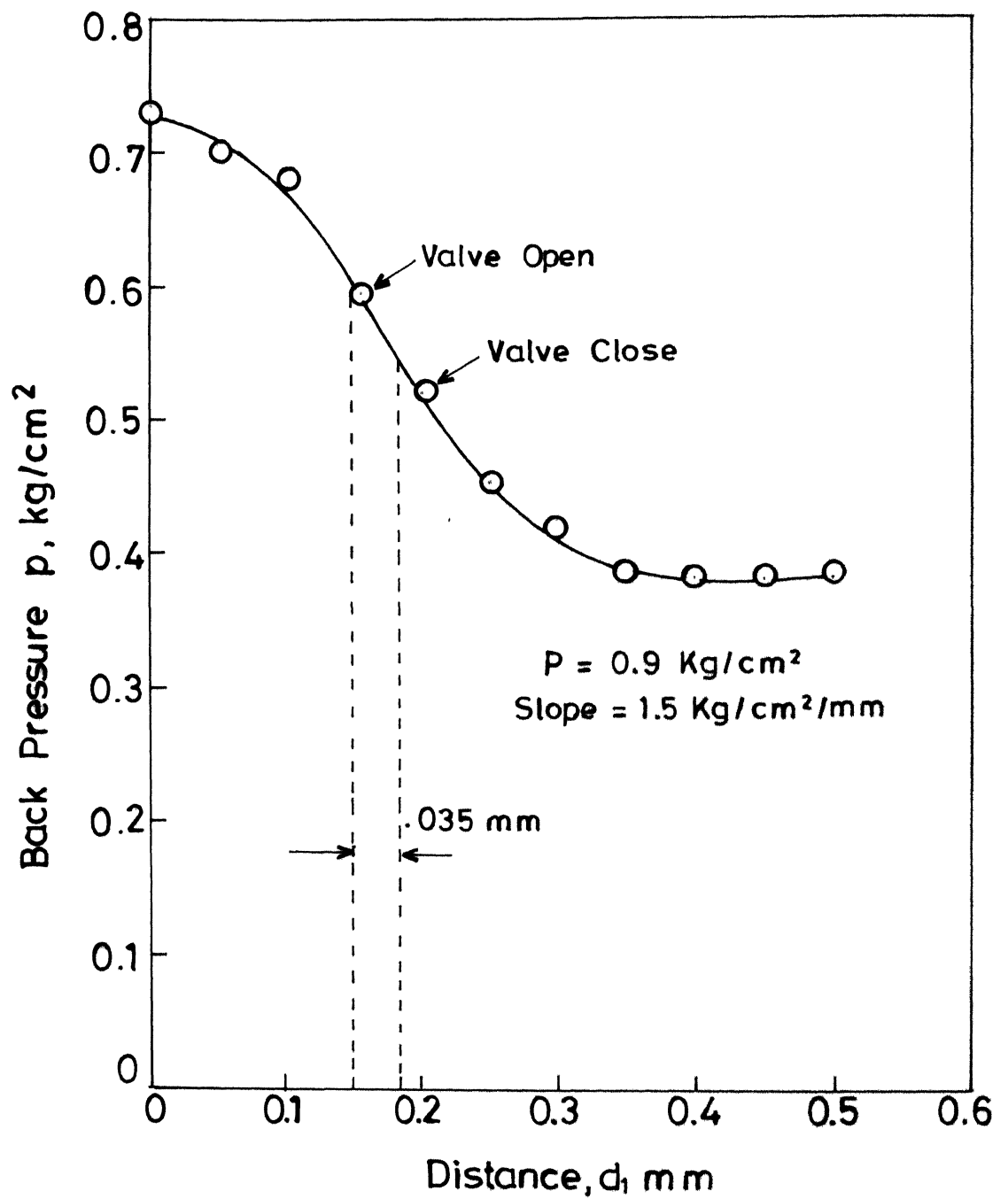


Fig.2.4 Characteristics of the Pneumatic Sensor.

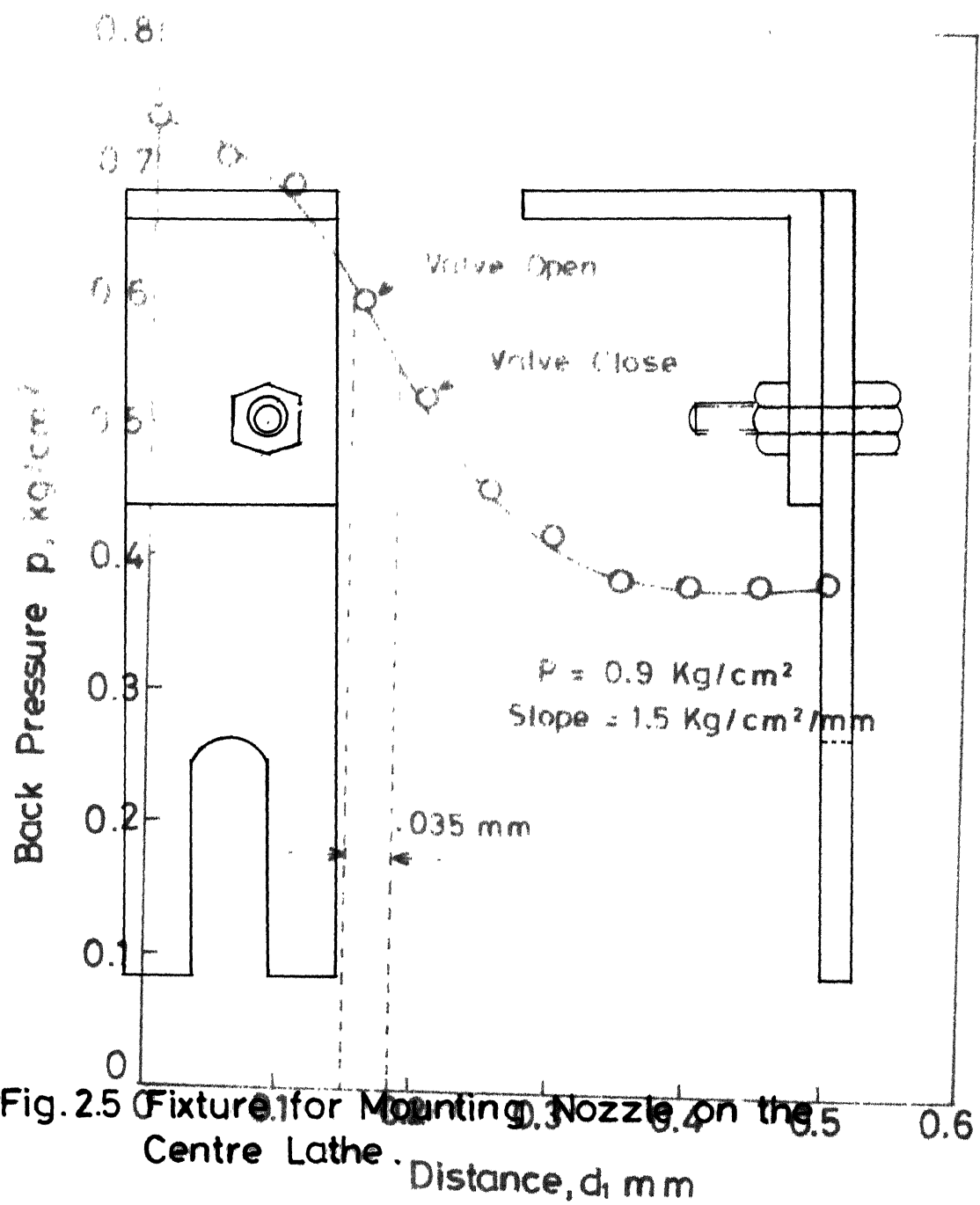


Fig. 2.5 Fixture for Mounting Nozzle on the Centre Lathe.

Fig. 2.4 Characteristics of the Pneumatic Sensor.



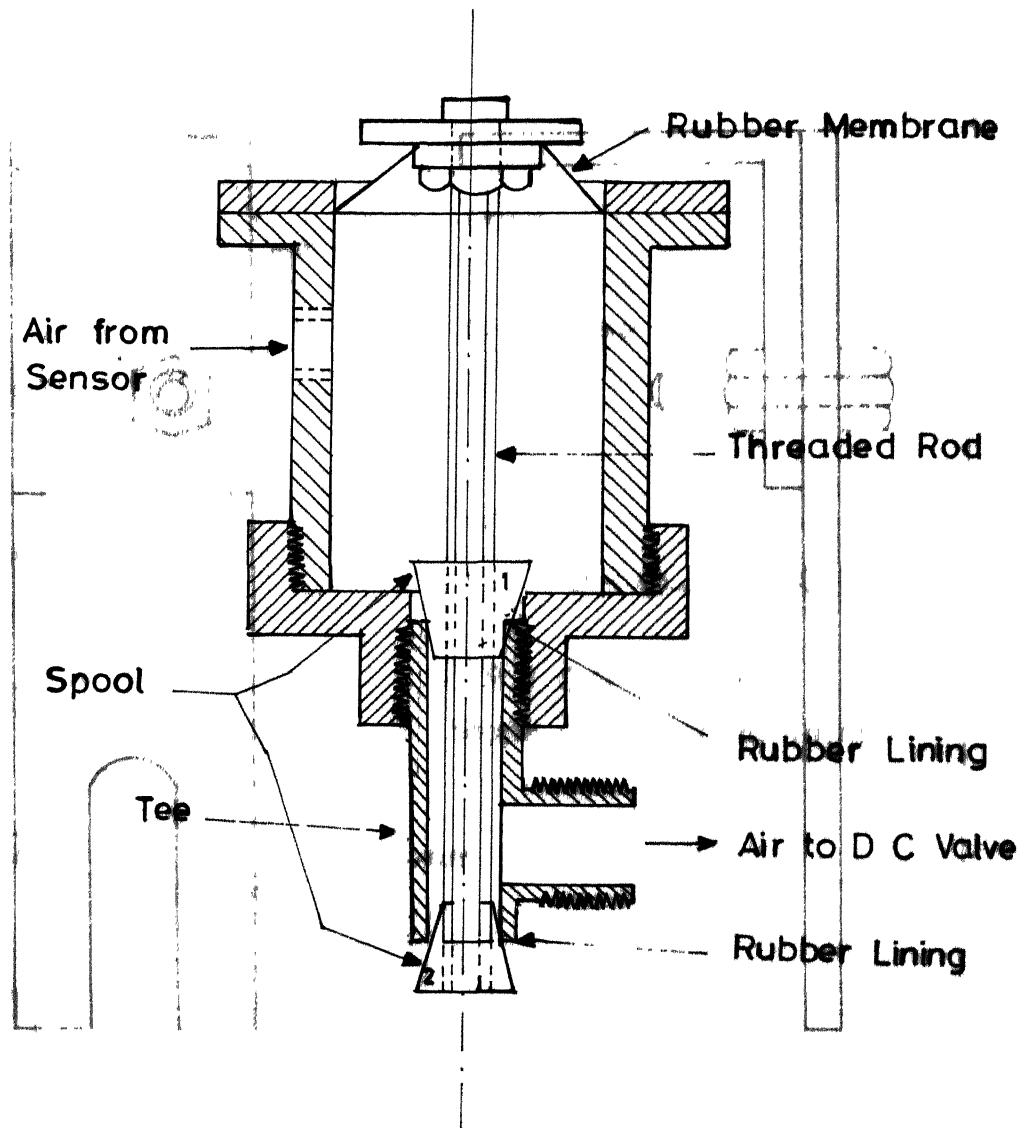


Fig.2.5 Fixture for Mounting Nozzle on the  
 Fig.2.6 Sensitivity Improving Device.

Fig. 2.6 Sensitivity Improving Device. The diagram shows a cross-section of a device with a central vertical passage. The passage is lined with rubber and contains a spool and a tee fitting. Air from a sensor enters from the left, and air to a DC valve exits to the right. The device is mounted on a base with a threaded rod passing through it.

However, in practice poorer sensitivity is achieved due to the curvature of the workpiece surface. From nozzle-orifice characteristics the sensitivity is found to be 0.035 mm. This sensitivity goes on increasing with the increase in the curvature of the workpiece surface.

The fixture for mounting the pneumatic sensor on the saddle of the centre lathe is shown in figure 2.5.

### 2.3 SENSITIVITY IMPROVING DEVICE :

The need to incorporate such device arises from the fact that the pilot-controlled direction control valve closes only at the pressure of  $0.2 \text{ kg/cm}^2$  and the pneumatic sensor characteristics show that for no obstruction-nozzle-tip distance the back pressure would be that low. It is not advisable to reduce input pressure in order to get  $0.2 \text{ kg/cm}^2$  from pneumatic sensor because the valve opens at  $0.6 \text{ kg/cm}^2$  and this pressure also must lie in the range of the pneumatic sensor output pressure signal.

The diagram of the sensitivity improving device is shown in figure 2.6. In the initial position the spool 1 is forced to rest on the rubber lining by the tension in the rubber membrane. Now as the compressed air enters the device it exerts force on the rubber membrane that tends to lift the spool 1 from the rubber lining and bring spool 2 in contact with the rubber lining, which is initially suitably

apart from the rubber lining. When pressure exceeds certain limit the force due to the pressure overcomes the tension of the membrane and lifts the spool 1 from its initial position and brings spool 2 in contact with the rubber lining. Hence the air flows out of the device and the pilot-controlled direction control valve is connected to the pneumatic sensor. Now if the pressure decreases again the tension in the membrane overcomes the force due to compressed air and spools 1 and 2 again come to their initial position. The pneumatic sensor and dc valve are disconnected in this position. The compressed air in the conduit between the sensitivity improving device and the direction control valve is allowed to flow out from the gap between the spool 2 and the rubber lining. Otherwise the air would have been trapped in the conduit and due to the pressure exerted by this air the valve would never have closed.

The pressure at which the air opens the device depends on the tension in the membrane which in-turn depends on the position of the spools. The spools can be shifted along the length of the threaded rod and the device can be adjusted for different pressures.

#### 2.4 PILOT-CONTROLLED DIRECTION CONTROL VALVE :

The need to incorporate the pilot-controlled direction control valve arises because the pressure required to actuate the tool is higher than the back-pressure available

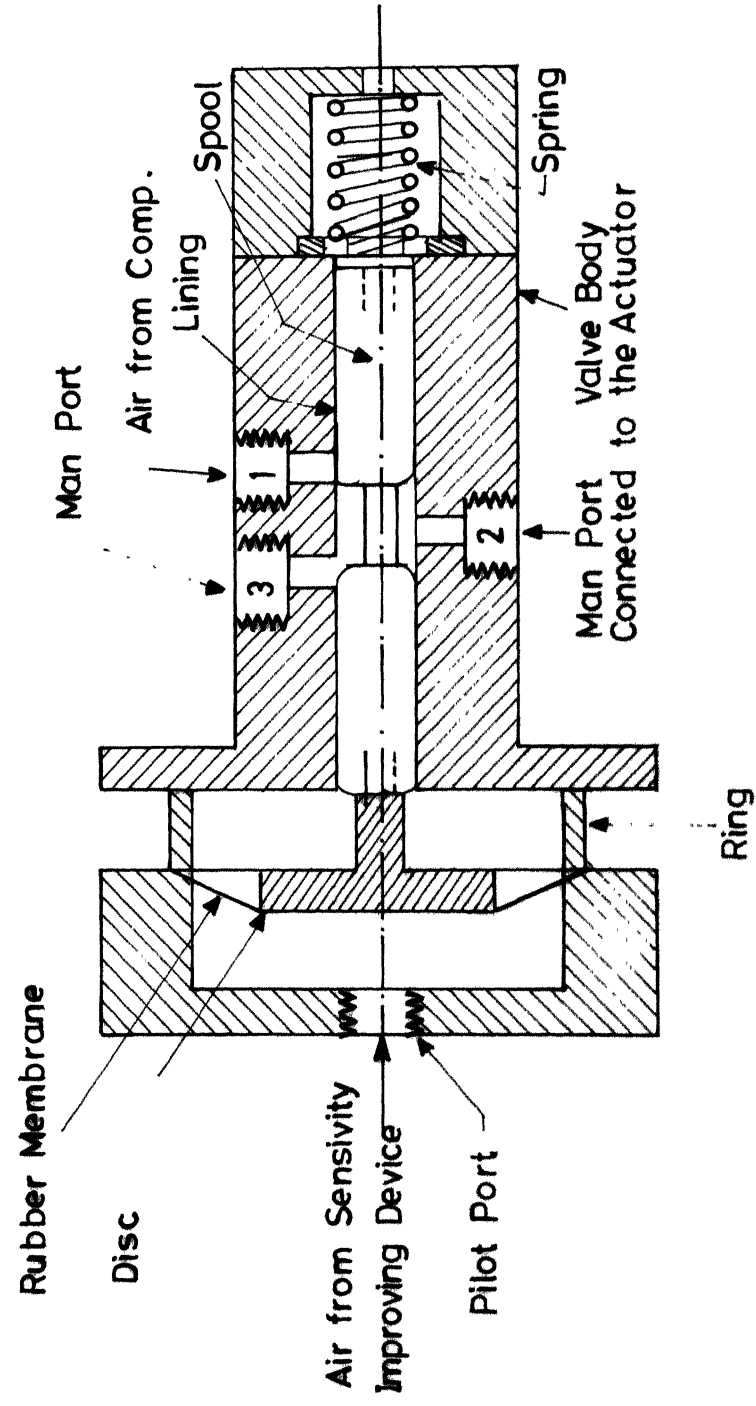


Fig. 2.7 Pilot Controlled Direction Control Valve .

from the pneumatic sensor. The valve uses the backpressure signal to connect and disconnect the actuator from the compressor surge tank which contains air at a high pressure.

The diagram of the pilot-controlled direction control valve is shown in figure 2.7. Initially when the force applied on the disc by the compressed air is not sufficient to overcome the spring force. The manport 2 is connected to the manport 3 which is open to the atmosphere. As the pressure acting on the disc exceeds certain limit, the force acting on the disc is sufficient to overcome the spring force and the frictional force between the lining and the spool the spool slides along the lining. Now the manport 2 is disconnected from the manport 3 and connected to the manport 1. The valve is said to be open now. This connects compressor surge tank to the actuator. Now as the pressure acting on the disc reduces again the spool again slides back to the initial position and the compressor is disconnected from the actuator. The compressed air in the conduit between the pilot-controlled direction control valve and the actuator flows out from the manport 3 as the manport 2 is again connected to the manport 3.

The pressure acting on the disc ranges from 0 to 1 kg/cm<sup>2</sup> whereas pressure acting on the actuator piston is of the order of 6.0 kg/cm<sup>2</sup>. The pilot-controlled direction control valve can give upto 10 kg/cm<sup>2</sup> to the actuator provided the compressor can supply the air at that pressure.

# PLAN

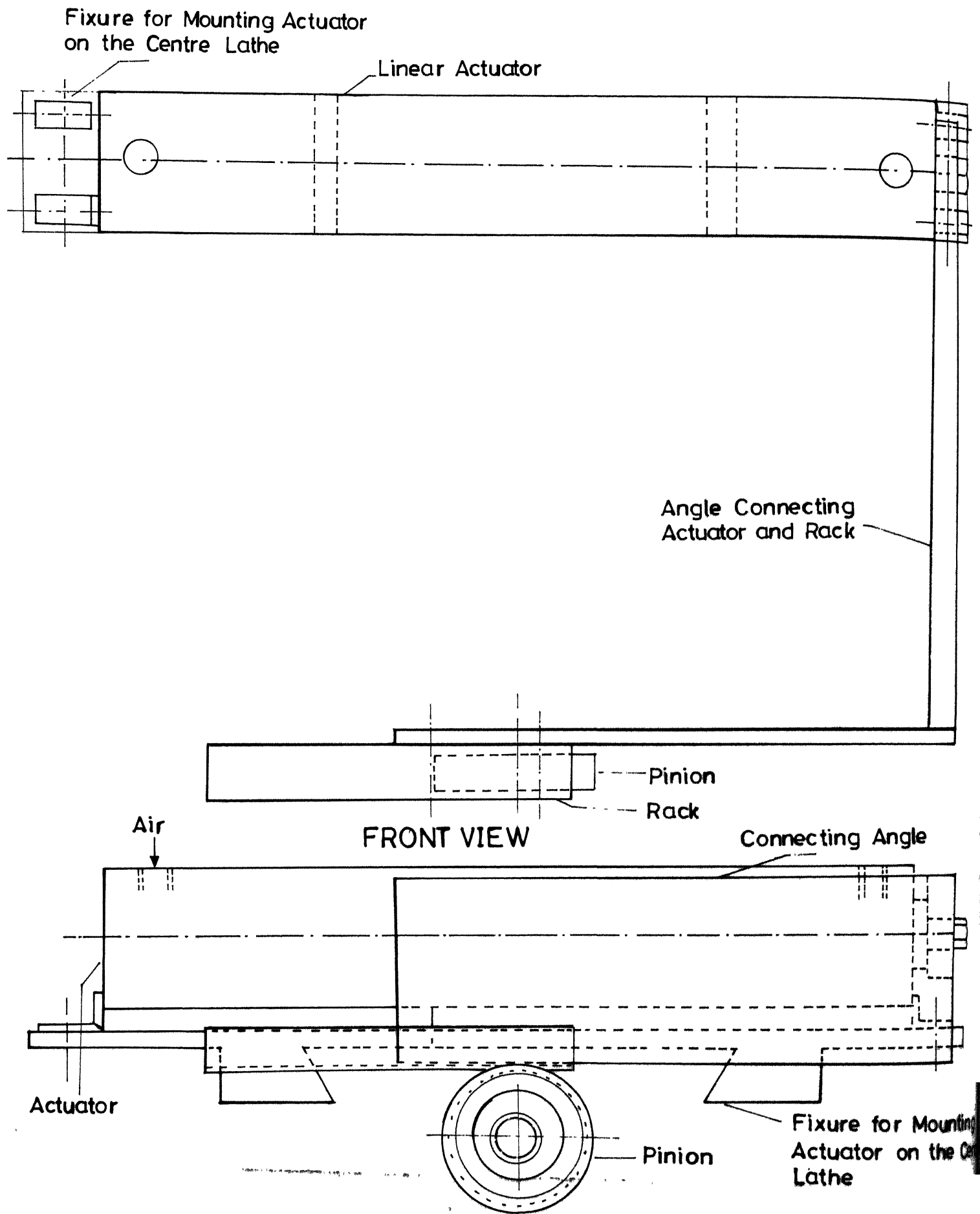


Fig. 2.8 Actuator Mechanism .

## 2.5 ACTUATION MECHANISM :

The actuation mechanism is required to convert the pneumatic pressure into the mechanical displacement of the tool.

The diagram of the actuation mechanism is shown in the figure 2.8. The fixture facilitates the mounting of the actuator on the lathe-structure. The dovetail of the fixture engages the dovetail of the lathe on which the cross-slide moves. The cross-slide is connected to the cross-feed screw. A pinion is mounted at the end of the cross-feed screw by removing the hand-wheel from there. The actuator-pistonrod is connected to the rack by a connecting angle. The fixture is mounted on the lathe-dovetail in such a way that the rack rests on the pinion.

As the compressed air enters the actuator cylinder it moves the piston which in-turn moves the rack. Due to the meshing of the rack and the pinion the pinion rotates. This causes the rotation of the cross-feed screw and the cross-slide moves towards the workpiece axis along with the tool.

## 2.6 FABRICATION OF THE EXPERIMENTAL SET-UP :

The nozzle and orifice of the pneumatic sensor were fabricated from the brass-rod on the centre-lathe and attached to a readymade tee joint of cast-steel to form a pneumatic sensor.

The sensitivity improving device was fabricated from the aluminium rod on the centre lathe. However the tee used was of cast steel.

The pilot-controlled direction control valve was purchased from the market. The spool is of stainless steel and the rest of the parts are of aluminium. An aluminium disc was made to replace the piston in order to reduce the friction.

A readily available linear actuator was used. The rack, pinion, connecting angle and fixture were fabricated on the milling-machine. The rack and pinion were of stainless steel where as the connecting angle and the fixture were made from MS plates.



## CHAPTER -III

### EXPERIMENTATION

#### 3.1 OBJECTIVE :

The objective of the experimentation was to test the experimental set-up designed and fabricated under different machining conditions. As the objective of the present work was to improve the dimensional stability a quantitative study of the reduction in the error is imperative.

#### 3.2 PARAMETERS :

The factors affecting the toolwear in metal-cutting are namely cutting-speed, feed, depth of cut, tool-material, work-material and tool-geometry. To test the set-up under different machining conditions cutting speed and feed were changed. The HSS tools were used to cut mildsteel. Tool-geometry was also kept same for every experiment. Details of the tool-geometry are given in the appendix -1. The depth of cut desirable was one that would give enough toolwear to be compensated. The depth of cut of approximately 0.5 mm was used for all the experiments.

The cutting-speed and feed were the two parameters that were varied during the experiments. But, it is very

difficult to control the cutting-speed precisely because cutting speed is affected by the rotational speed of the workpiece as well as the work-diameter. During the experiments the rotational speed was varied between 1000 rpm to 500 rpm and the work-diameter change from 36.7 mm to 20.6mm. This gave a cutting-speed range of 114 m/min to 33 m/min. This range is appropriate since very high cutting speed would result in excessive vibrations and very low cutting speed would not give sufficient wear to compensate. Four rotational speeds used were 1000 rpm, 800 rpm, 640 rpm and 500 rpm. For each rotational speed four feeds were used, 0.05 mm/rev, 0.063 mm/rev., 0.081 mm/rev. and 0.1 mm/rev. Totally sixteen experiments were conducted and the set-up was tested for a range of speed and feed.

### 3.3 PREPARATIONS :

The experimental set-up was assembled and mounted on the HMT LB-17 centre lathe for which it was designed and fabricated. The details of the machine-tool are given in the appendix-2.

The pneumatic sensor was mounted on the saddle of the machine-tool so that it would travel along the length of the workpiece with the tool. The nozzle axis was adjusted in the same plane as the lathe axis. The nozzle would lag behind

the tool to avoid any physical contact with the unmachined part of the workpiece. The position of the nozzle would not be affected by the transverse motion of the cross-slide.

Sixteen cutting edges were prepared according to the required cutting tool-geometry. A mildsteel rod of about 38 mm diameter and 350 mm length was prepared for being used as a workpiece. The workpiece was held between the centres to avoid vibrations caused by inaccuracies in holding by chuck. Some preliminary cuts were taken to remove eccentricity in the workpiece.

#### 3.4 PROCEDURE :

Basic experimentation consisted of taking a 30.0 cm. long cut with the feedback provided by the experimental set-up for a particular machining condition and then repeating the cut with identical machining condition without feed back.

Following procedure was followed for taking cut with feedback.

The compressor was run until pressure of  $6.0 \text{ kg/cm}^2$  was built in the surge tank. This ensured constant input pressure of  $0.9 \text{ kg/cm}^2$  during the cut. The diameter of the workpiece was measured with a micrometer and the tool was set for 0.5 mm depth of cut. The cut was taken for 1.0 cm length and the cutting was interrupted. The conduit connecting the pneumatic sensor to the sensitivity improving device was

disconnected from the sensitivity improving device and connected to a pressure gauge. The compressor was switched on and the nozzle was brought in contact with machined workpiece surface. The input pressure to the pneumatic sensor was adjusted such that the backpressure was  $0.75 \text{ kg/cm}^2$ . This ensures constant input pressure of  $0.9 \text{ kg/cm}^2$  for all the experiments. The position of the nozzle was adjusted to give backpressure just below  $0.55 \text{ kg/cm}^2$ . This means that the sensitivity improving device was about to open with the slight increament of the backpressure. The pressure gauge was disconnected and the conduit was again connected to the sensitivity improving device. A limit to the cross-slide motion towards the workpiece axis was provided by the arrangement in the machine tool itself. This was necessary because of the lag between the tool and the nozzle. This fixed the maximum compensation which depended on the sensitivity of the experimental set-up. Slight over-shoot was given to ensure closure of the valve. The second opening of the compressor surge tank was opened and the cut was taken for 30.0 cm length. The compensation was observed during the cut. After the cut a dial indicator was attached to the cross-slide and the stylus was brought in contact with the workpiece surface at the height of the lathe-axis. The stylus was brought at the starting point of the cut and the dial indicator

reading was adjusted to zero. The dial indicator was traversed along the length of the workpiece with the cross-slide and reading was taken at every 1.0 cm. The reading gives the error in the radius. The dial indicator was removed and the next cut was taken with a new cutting edge.

After conducting sixteen experiments the set-up was dismounted and the cutting edges were photographed using a microscopic camera. The tools were reground and with identical cutting conditions but without feedback sixteen cuts were repeated and the dial indicator readings taken.

## CHAPTER - IV

### RESULTS, DISCUSSION, CONCLUSION AND SCOPE FOR FUTURE WORK

#### 4.1 RESULTS :

The results obtained from the sixteen experiments with feedback and sixteen experiments without feedback are tabulated in table 1 to 16. Results obtained for the same machining conditions with feedback system and without feedback system are tabulated in the same table.

Sixteen graphs of error in the radius against the length of cut were plotted using LOTUS package. Figures 4.1 to 4.16 shows the graphs corresponding to the experiment 1 to 16 in that order.

From the obtained error in the radius from experiments with and without feedback system the coefficient of error reduction (E) was calculated for each experiment. Where

$$E = \left( 1 - \frac{\text{Error with feedback}}{\text{Error without feedback}} \right)$$

These results are tabulated separately in table 17. The microscopic photographs of the tools used in the experiments are shown in Figure 4.17 to Fig. 4.20. Tool is given number according to the number of the experiment in which it was used. Magnification is of the order of 200.

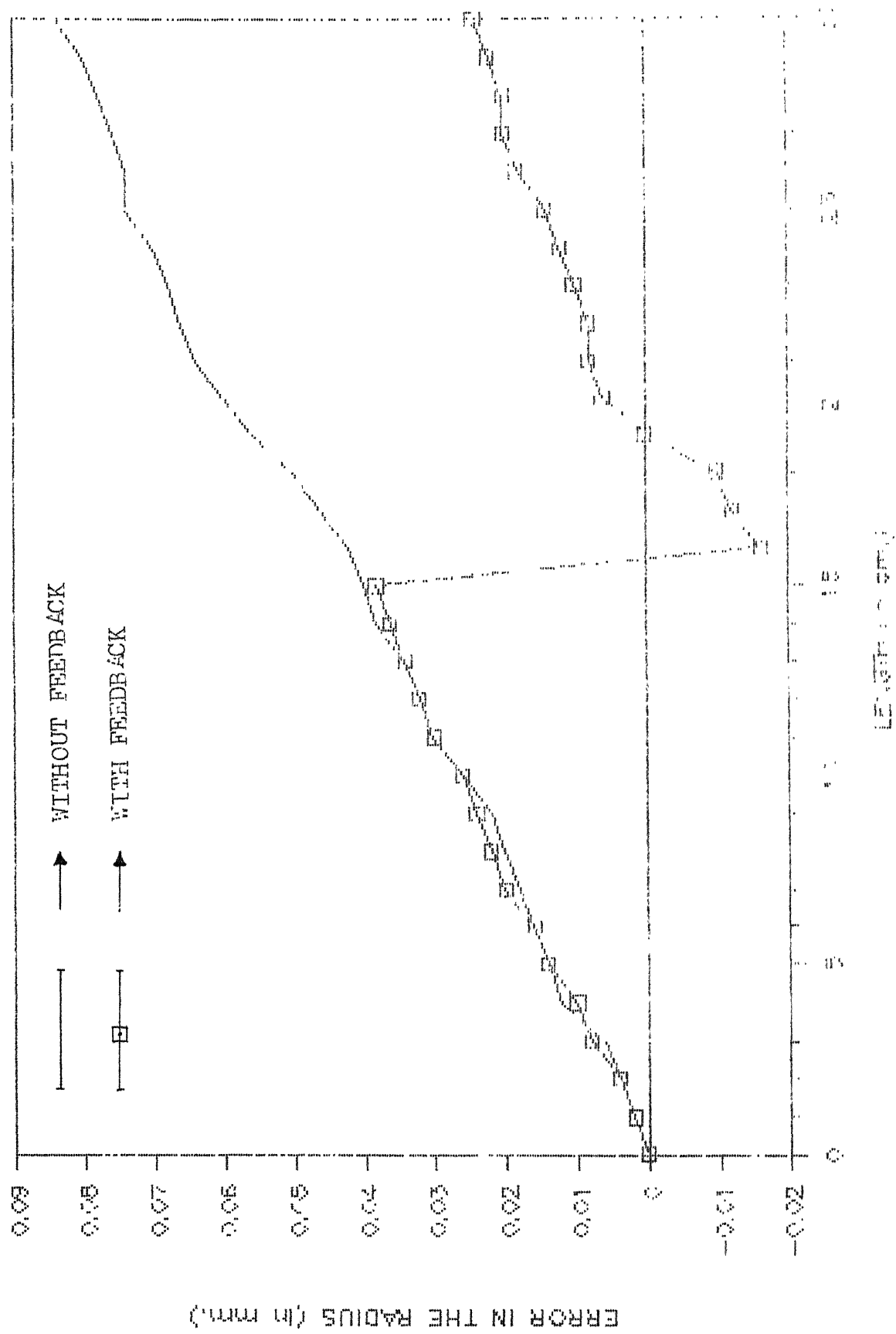


Fig. 4.1 Graph showing results of experiment -1

EXPERIMENT -1

Rotational Speed = 1000 rpm.

Feed = 0.05 mm/rev.

Original diameter = 36.70 mm

Desired diameter = 35.76 mm

Cutting Speed = 114 m/min

TABLE -1

Results of experiment -1

Dr. No.	Position along the length of cut cm.	Error in the radius with feedback mm.	Error in the Radius without feedback mm.
1	0.0	0.0	0.0
2	1.0	0.002	0.002
3	2.0	0.004	0.004
4	3.0	0.008	0.006
5	4.0	0.01	0.012
6	5.0	0.014	0.014
7	6.0	0.016	0.016
8	7.0	0.02	0.018
9	8.0	0.022	0.02
10	9.0	0.024	0.022
11	10.0	0.026	0.026
12	11.0	0.030	0.03
13	12.0	0.032	0.032
14	13.0	0.034	0.034
15	14.0	0.036	0.038
16	15.0	0.038	0.04
17	16.0	-0.016	0.042
18	17.0	-0.012	0.046
19	18.0	-0.01	0.05
20	19.0	0.000	0.056
21	20.0	0.006	0.06
22	21.0	0.008	0.064
23	22.0	0.008	0.066
24	23.0	0.01	0.068
25	24.0	0.012	0.07
26	25.0	0.014	0.074
27	26.0	0.018	0.074
28	27.0	0.02	0.076
29	28.0	0.02	0.078
30	29.0	0.022	0.08
31	30.0	0.024	0.084



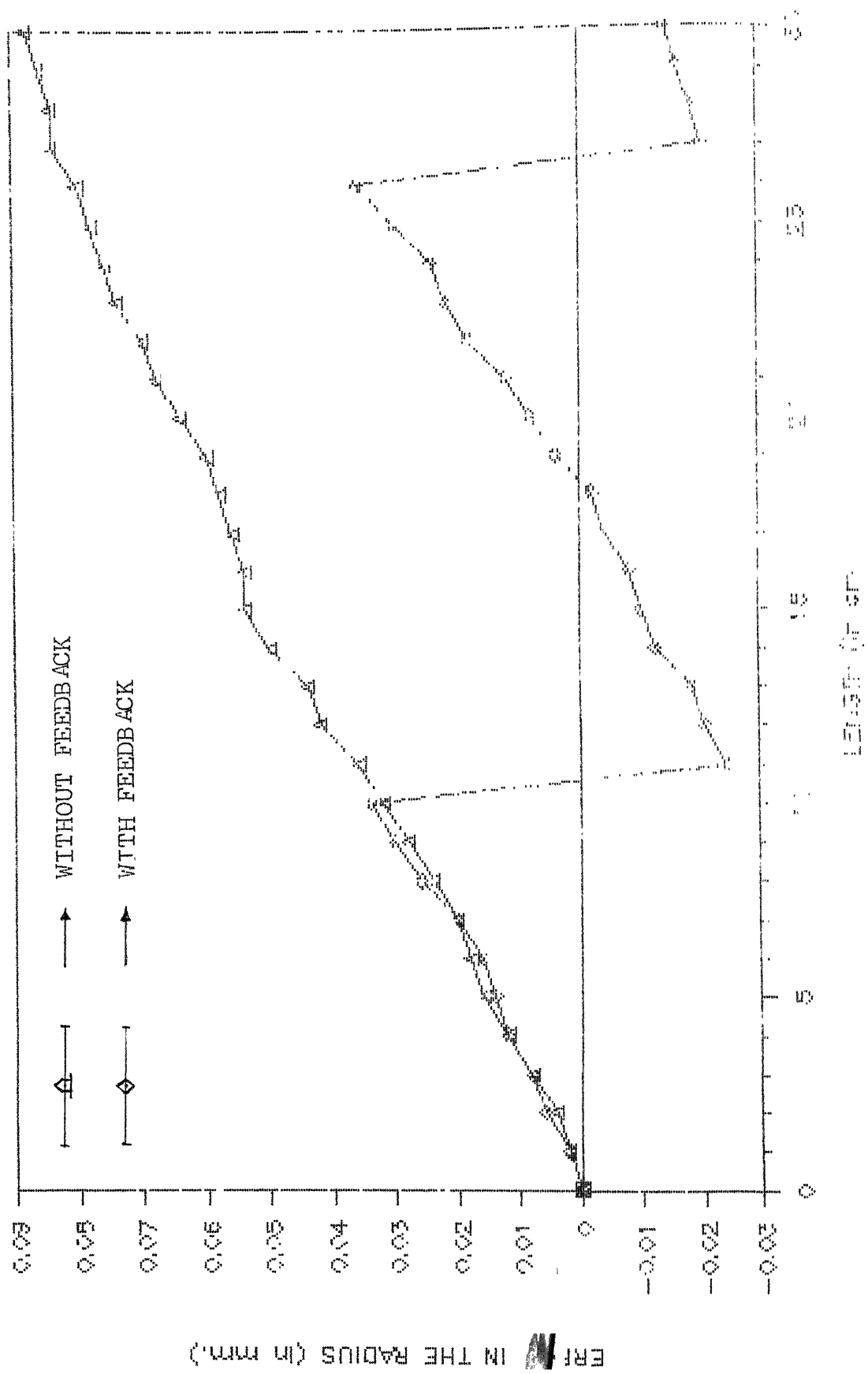


Fig. 4.2 Graph showing results of experiment -2

EXPERIMENT -2

Rotational Speed = 1000 rpm  
 Feed = 0.063 mm/rev.  
 Original diameter = 35.76 mm  
 Desired diameter = 34.74 mm  
 Cutting Speed = 111 m/min.

TABLE -2

Results of experiment -2

Sr. No.	Position along the length of cut cm.	Error in the radius with feedback mm.	Error in the Radius without feedback mm.
1	0.0	0.0	0.0
2	1.0	0.002	0.002
3	2.0	0.006	0.004
4	3.0	0.008	0.008
5	4.0	0.012	0.012
6	5.0	0.014	0.016
7	6.0	0.016	0.018
8	7.0	0.02	0.02
9	8.0	0.026	0.024
10	9.0	0.03	0.028
11	10.0	0.034	0.032
12	11.0	-0.024	0.036
13	12.0	-0.02	0.042
14	13.0	-0.018	0.044
15	14.0	-0.012	0.05
16	15.0	-0.01	0.054
17	16.0	-0.008	0.054
18	17.0	-0.004	0.056
19	18.0	-0.002	0.058
20	19.0	0.004	0.06
21	20.0	0.008	0.064
22	21.0	0.012	0.068
23	22.0	0.018	0.07
24	23.0	0.022	0.074
25	24.0	0.024	0.076
26	25.0	0.03	0.078
27	26.0	0.036	0.08
28	27.0	-0.02	0.084
29	28.0	-0.018	0.084
30	29.0	-0.016	0.086
31	30.0	-0.014	0.088

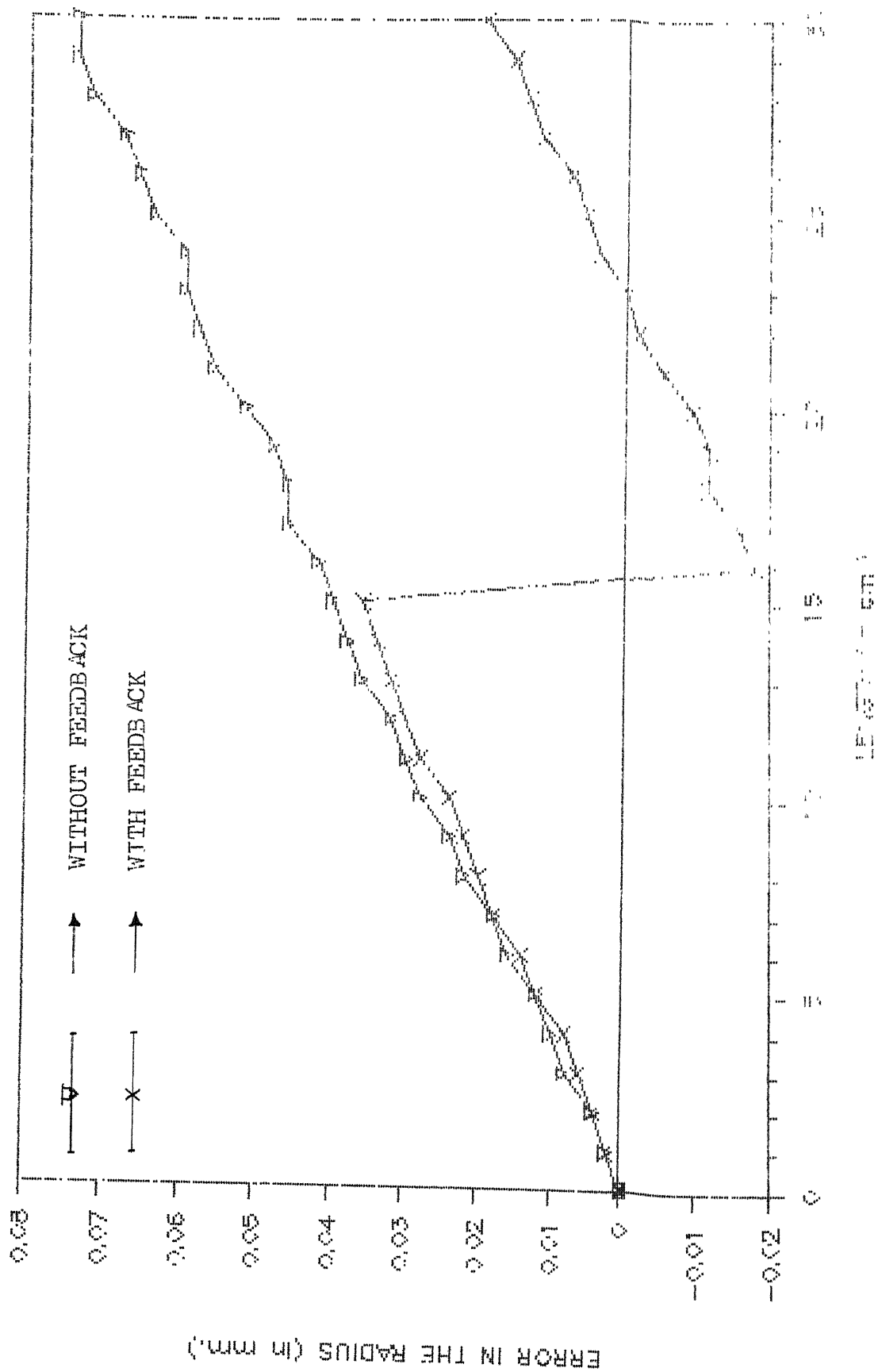


Fig. 4.3 Graph showing results of experiment -3

EXPERIMENT -3

Rotational Speed = 1000rpm  
 Feed = 0.081 mm/rev.  
 Original diameter = 34.74 mm/rev.  
 Desired diameter = 33.70 mm  
 Cutting Speed = 108 m/min.

TABLE -3

Results of experiment -3

Sr. No.	Position along the length of cut cm.	Error in the radius with feedback mm.	Error in the Radius without feedback mm.
1	0.0	0.0	0.0
2	1.0	0.002	0.002
3	2.0	0.004	0.004
4	3.0	0.006	0.008
5	4.0	0.008	0.01
6	5.0	0.012	0.012
7	6.0	0.014	0.016
8	7.0	0.018	0.018
9	8.0	0.02	0.022
10	9.0	0.022	0.024
11	10.0	0.024	0.028
12	11.0	0.028	0.03
13	12.0	0.03	0.032
14	13.0	0.032	0.036
15	14.0	0.034	0.038
16	15.0	0.036	0.04
17	16.0	-0.018	0.042
18	17.0	-0.016	0.046
19	18.0	-0.012	0.046
20	19.0	-0.012	0.048
21	20.0	-0.01	0.052
22	21.0	-0.006	0.056
23	22.0	-0.002	0.058
24	23.0	0.000	0.06
25	24.0	0.004	0.06
26	25.0	0.006	0.064
27	26.0	0.008	0.066
28	27.0	0.012	0.068
29	28.0	0.014	0.072
30	29.0	0.016	0.074
31	30.0	0.02	0.074

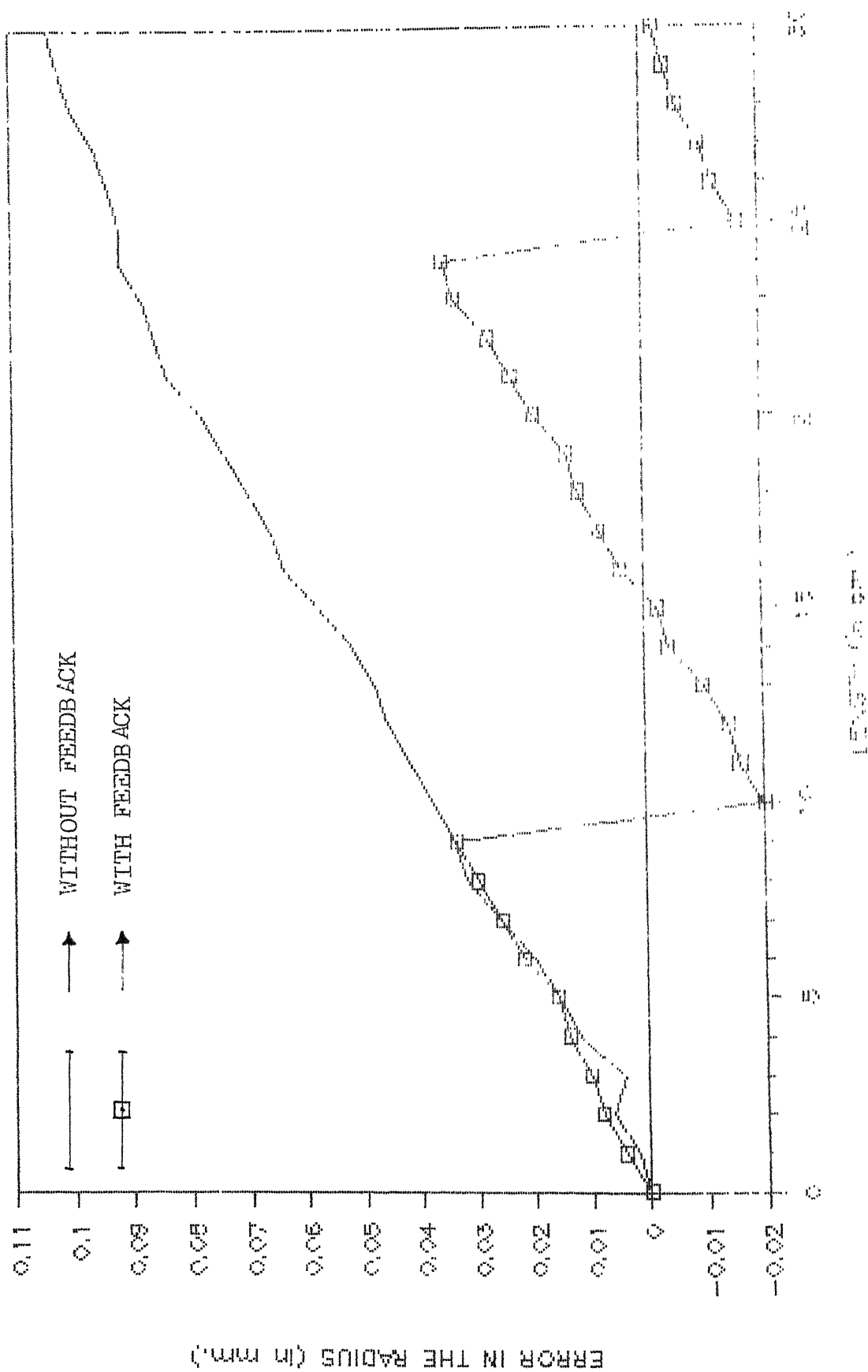


Fig. 4.4 Graph showing results of experiment -4

EXPERIMENT -4

Rotational Speed = 1000rpm  
 Feed = 0.1 mm/rev.  
 Original diameter = 33.70 mm.  
 Desired diameter = 32.66 mm  
 Cutting Speed = 104 m/min.

TABLE -4

Results of experiment -4

Sr. No.	Position along the length of cut cm.	Error in the radius with feedback mm.	Error in the Radius without feedback mm.
1	0.0	0.0	0.0
2	1.0	0.004	0.002
3	2.0	0.008	0.006
4	3.0	0.01	0.004
5	4.0	0.014	0.012
6	5.0	0.016	0.016
7	6.0	0.022	0.02
8	7.0	0.026	0.026
9	8.0	0.03	0.032
10	9.0	0.034	0.034
11	10.0	-0.02	0.038
12	11.0	-0.016	0.042
13	12.0	-0.014	0.046
14	13.0	-0.01	0.048
15	14.0	-0.004	0.052
16	15.0	-0.002	0.058
17	16.0	0.004	0.064
18	17.0	0.008	0.066
19	18.0	0.012	0.07
20	19.0	0.014	0.074
21	20.0	0.02	0.078
22	21.0	0.024	0.084
23	22.0	0.028	0.086
24	23.0	0.034	0.088
25	24.0	0.036	0.092
26	25.0	-0.016	0.092
27	26.0	-0.012	0.094
28	27.0	-0.01	0.096
29	28.0	-0.006	0.1
30	29.0	-0.004	0.102
31	30.0	-0.002	0.104

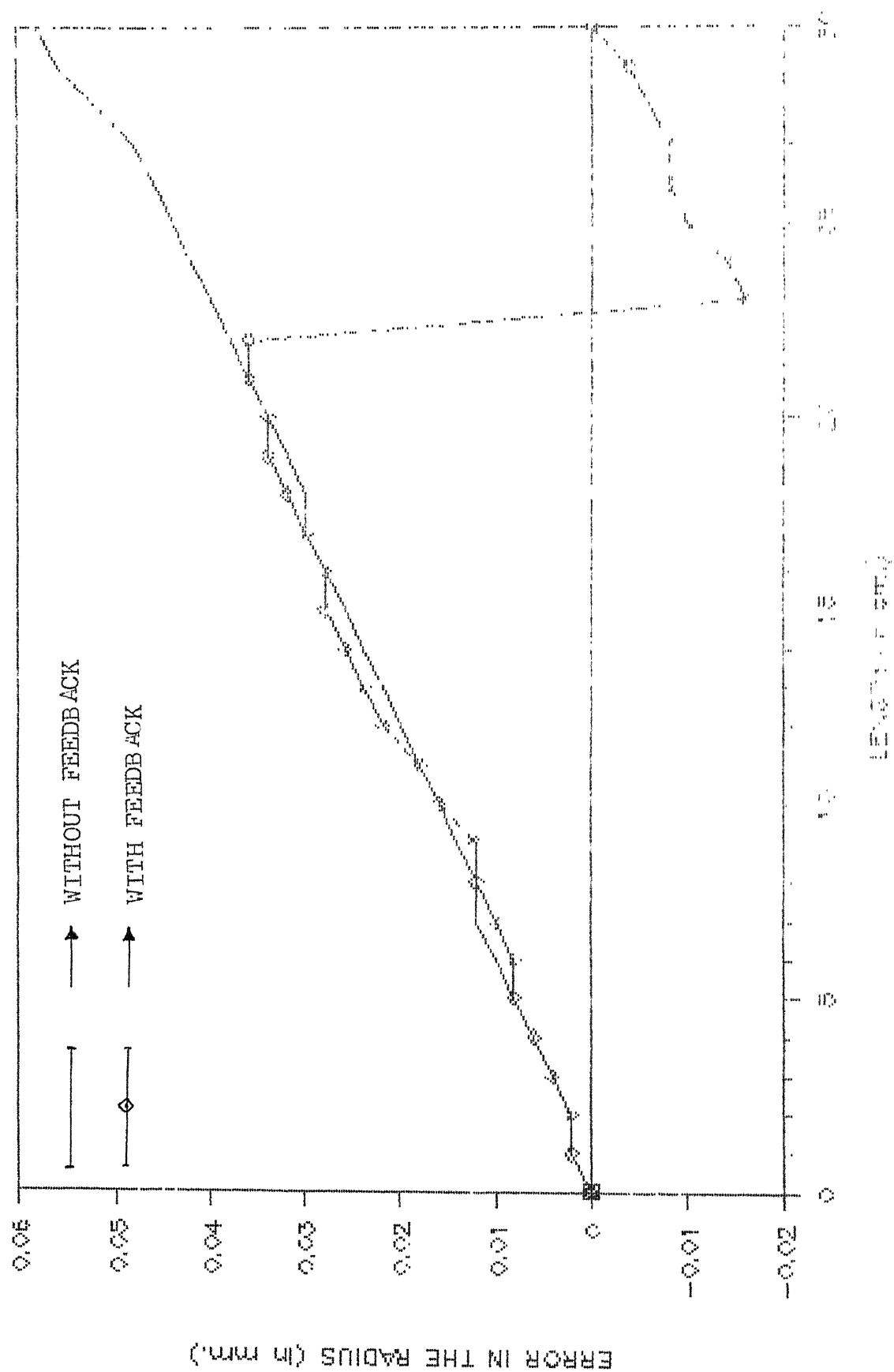


Fig. 4.5 Graph showing results of experiment 4.5

EXPERIMENT -5

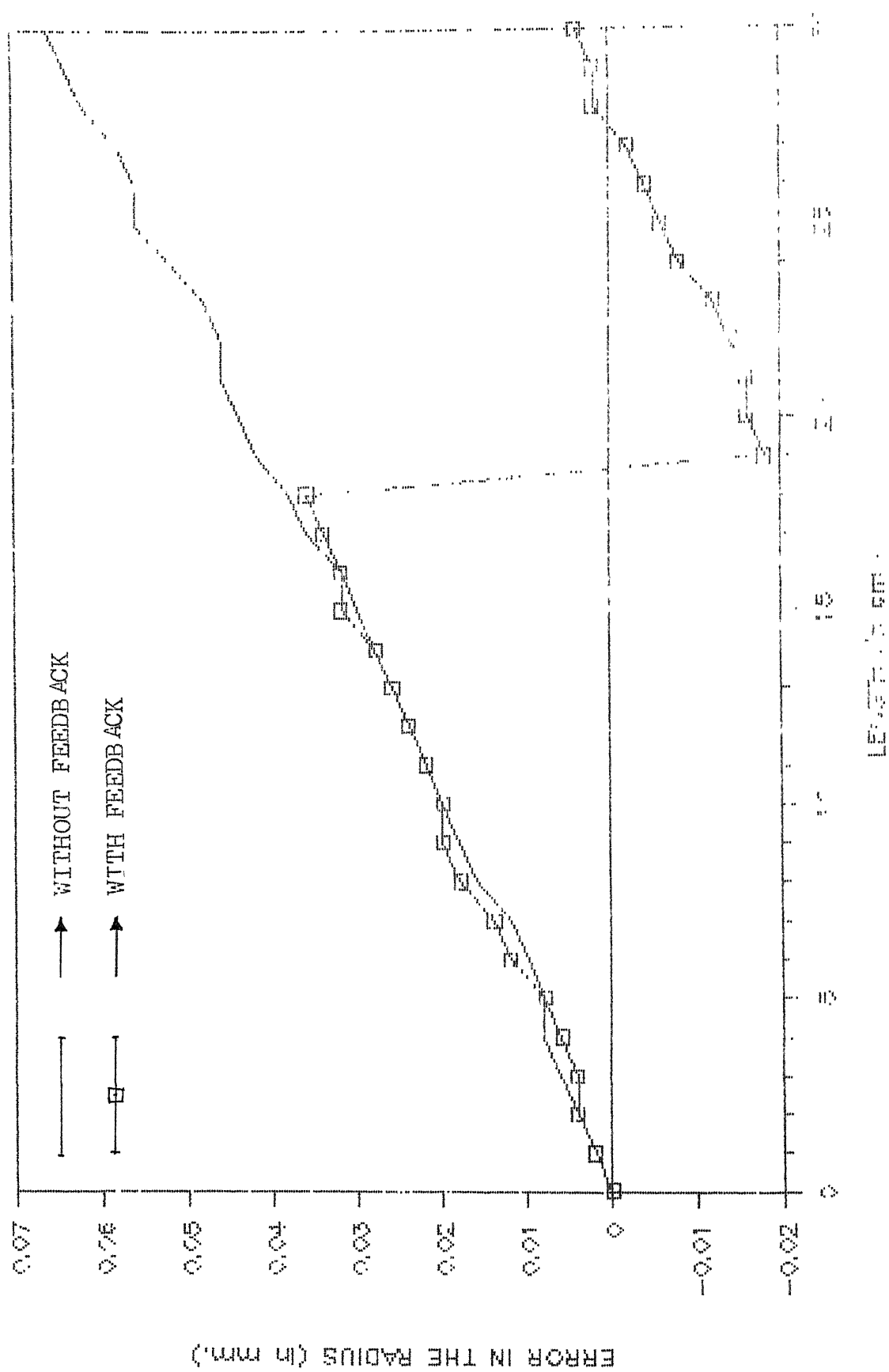
Rotational Speed = 800 rpm  
 Feed = 0.05 mm/rev.  
 Original diameter = 32.66 mm  
 Desired diameter = 31.62 mm  
 Cutting Speed = 81 m/min.

TABLE -5

Results of experiment -5

Dr.No.	Position along the length of cut cm.	Error in the radius with feedback mm.	Error in the Radius without feedback mm.
1	0.0	0.0	0.0
2	1.0	0.002	0.002
3	2.0	0.002	0.002
4	3.0	0.004	0.004
5	4.0	0.006	0.006
6	5.0	0.008	0.008
7	6.0	0.008	0.01
8	7.0	0.010	0.012
9	8.0	0.012	0.012
10	9.0	0.012	0.014
11	10.0	0.016	0.016
12	11.0	0.018	0.018
13	12.0	0.022	0.02
14	13.0	0.024	0.022
15	14.0	0.026	0.024
16	15.0	0.028	0.026
17	16.0	0.028	0.028
18	17.0	0.03	0.03
19	18.0	0.032	0.03
20	19.0	0.034	0.032
21	20.0	0.034	0.034
22	21.0	0.036	0.036
23	22.0	0.036	0.038
24	23.0	-0.016	0.04
25	24.0	-0.014	0.042
26	25.0	-0.01	0.044
27	26.0	-0.008	0.046
28	27.0	-0.008	0.048
29	28.0	-0.006	0.052
30	29.0	-0.004	0.056
31	30.0	0.000	0.058





Fi . 4.6 Graph showing results of experiment -6

EXPERIMENT -6

Rotational Speed = 800 rpm  
 Feed = 0.063 mm/rev.  
 Original diameter = 31.62 mm  
 Desired diameter = 30.62 mm  
 Cutting Speed = 78 m/min

TABLE -6

Results of experiment -6

Sr. No.	Position along the length of cut cm.	Error in the radius with feedback mm	Error in the Radius without feedback mm.
1	0.0	0.0	0.0
2	1.0	0.002	0.002
3	2.0	0.004	0.004
4	3.0	0.004	0.006
5	4.0	0.006	0.008
6	5.0	0.008	0.008
7	6.0	0.012	0.01
8	7.0	0.014	0.012
9	8.0	0.018	0.016
10	9.0	0.02	0.018
11	10.0	0.02	0.02
12	11.0	0.022	0.022
13	12.0	0.024	0.024
14	13.0	0.026	0.026
15	14.0	0.028	0.028
16	15.0	0.032	0.03
17	16.0	0.032	0.032
18	17.0	0.034	0.036
19	18.0	0.036	0.038
20	19.0	-0.018	0.042
21	20.0	-0.016	0.044
22	21.0	-0.016	0.046
23	22.0	-0.014	0.046
24	23.0	-0.012	0.048
25	24.0	-0.008	0.052
26	25.0	-0.006	0.056
27	26.0	-0.004	0.056
28	27.0	-0.002	0.058
29	28.0	0.002	0.062
30	29.0	0.002	0.064
31	30.0	0.004	0.066

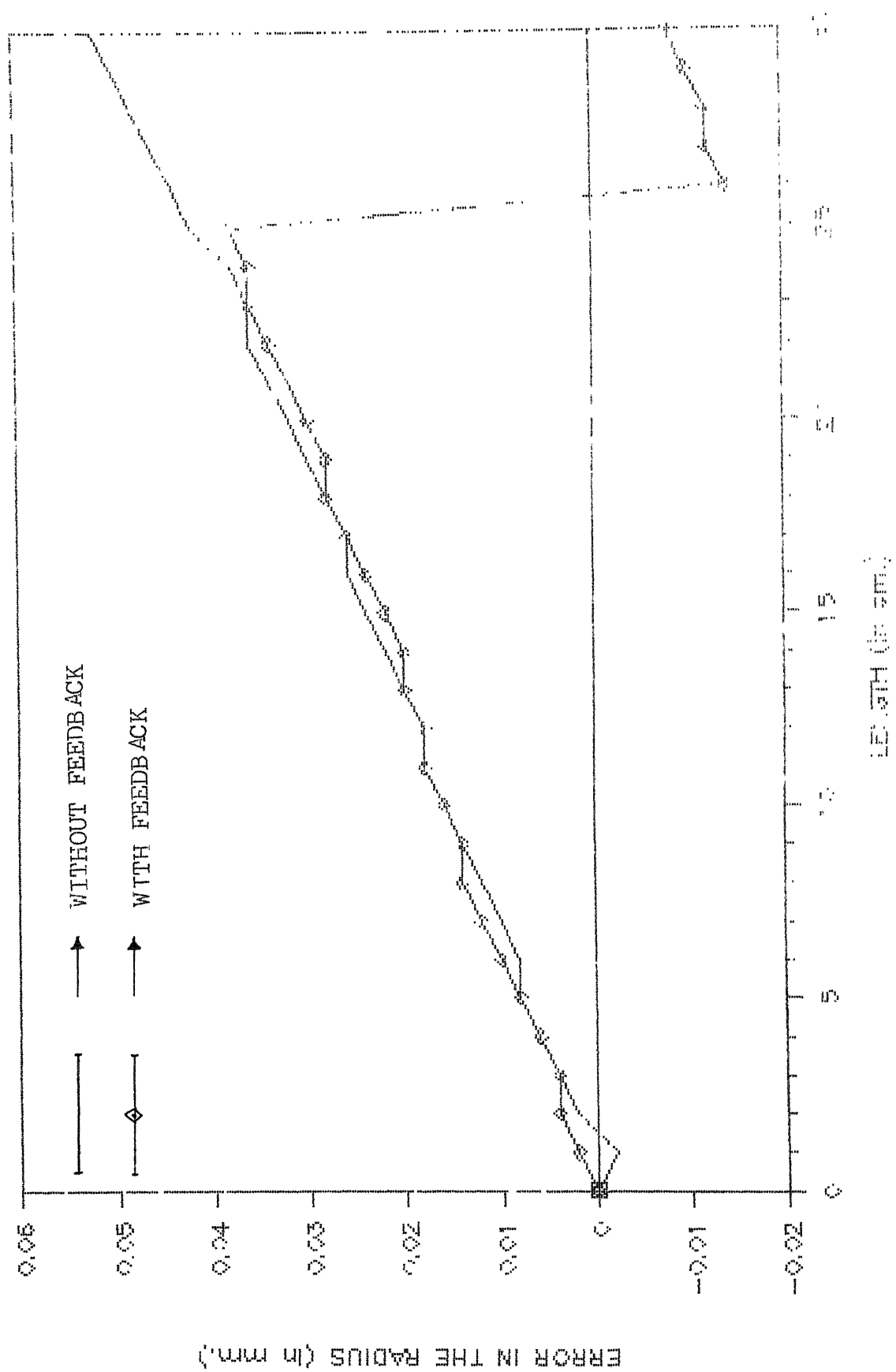


Fig. 4.7 Graph showing results of experiment -7

EXPERIMENT -7

Rotational Speed = 800 rpm  
 Feed = 0.081 mm/rev.  
 Original diameter = 30.62 mm  
 Desired diameter = 29.60 mm  
 Cutting Speed = 76 m/min.

TABLE -7

Results of experiment -7

Cr. No.	Position along the length of cut cm.	Error in the radius with feedback mm	Error in the Radius without feedback mm.
1	0.0	0.0	0.0
2	1.0	0.002	-0.002
3	2.0	0.004	0.002
4	3.0	0.004	0.004
5	4.0	0.006	0.006
6	5.0	0.008	0.008
7	6.0	0.01	0.008
8	7.0	0.012	0.01
9	8.0	0.014	0.012
10	9.0	0.014	0.014
11	10.0	0.016	0.016
12	11.0	0.018	0.018
13	12.0	0.018	0.018
14	13.0	0.02	0.02
15	14.0	0.02	0.022
16	15.0	0.022	0.024
17	16.0	0.024	0.026
18	17.0	0.026	0.026
19	18.0	0.028	0.028
20	19.0	0.028	0.03
21	20.0	0.03	0.032
22	21.0	0.032	0.034
23	22.0	0.034	0.036
24	23.0	0.036	0.036
25	24.0	0.036	0.038
26	25.0	0.038	0.042
27	26.0	0.014	0.044
28	27.0	-0.012	0.046
29	28.0	-0.012	0.048
30	29.0	-0.01	0.05
31	30.0	-0.008	0.052

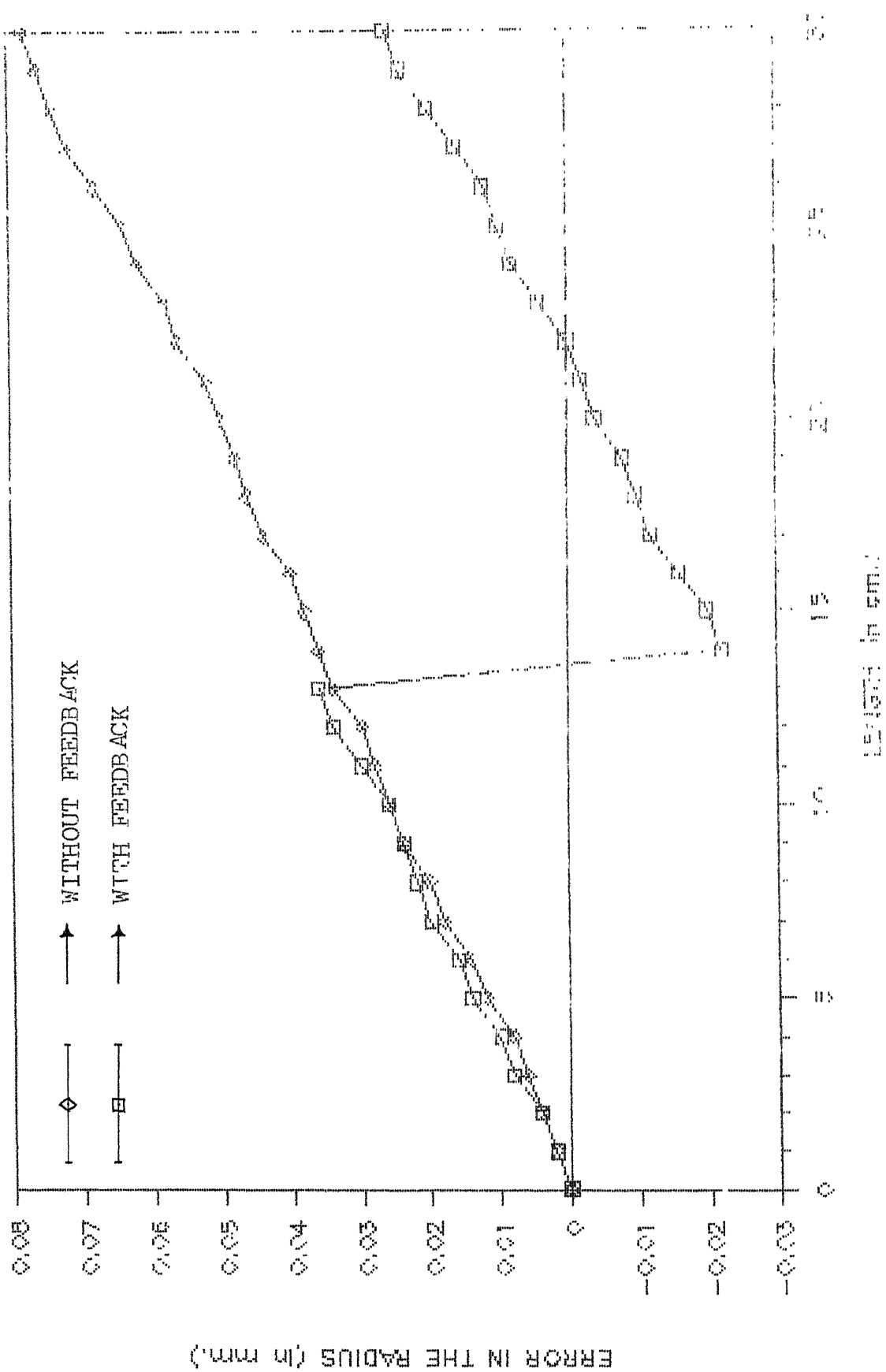


Fig. 4.8 Graph showing results of experiment -8

EXPERIMENT -8

Rotational Speed = 800 rpm

Feed = 0.063 mm/rev.

Original diameter = 29.60 mm

Desired diameter = 28.58 mm

Cutting speed = 73 m/min.

TABLE -8

Results of experiment -8

Dr. No.	Position along the length of cut cm.	Error in the radius with feedback mm	Error in the Radius without feedback mm.
1	0.0	0.0	0.0
2	1.0	0.002	0.002
3	2.0	0.004	0.004
4	3.0	0.008	0.006
5	4.0	0.01	0.008
6	5.0	0.014	0.012
7	6.0	0.016	0.014
8	7.0	0.02	0.018
9	8.0	0.022	0.02
10	9.0	0.024	0.024
11	10.0	0.026	0.026
12	11.0	0.03	0.028
13	12.0	0.034	0.03
14	13.0	0.036	0.034
15	14.0	-0.022	0.036
16	15.0	-0.02	0.038
17	16.0	-0.016	0.04
18	17.0	-0.012	0.044
19	18.0	-0.01	0.046
20	19.0	-0.008	0.048
21	20.0	-0.004	0.05
22	21.0	-0.002	0.052
23	22.0	0.000	0.056
24	23.0	0.004	0.058
25	24.0	0.008	0.062
26	25.0	0.01	0.064
27	26.0	0.012	0.068
28	27.0	0.016	0.072
29	28.0	0.02	0.074
30	29.0	0.024	0.076
31	30.0	0.026	0.078

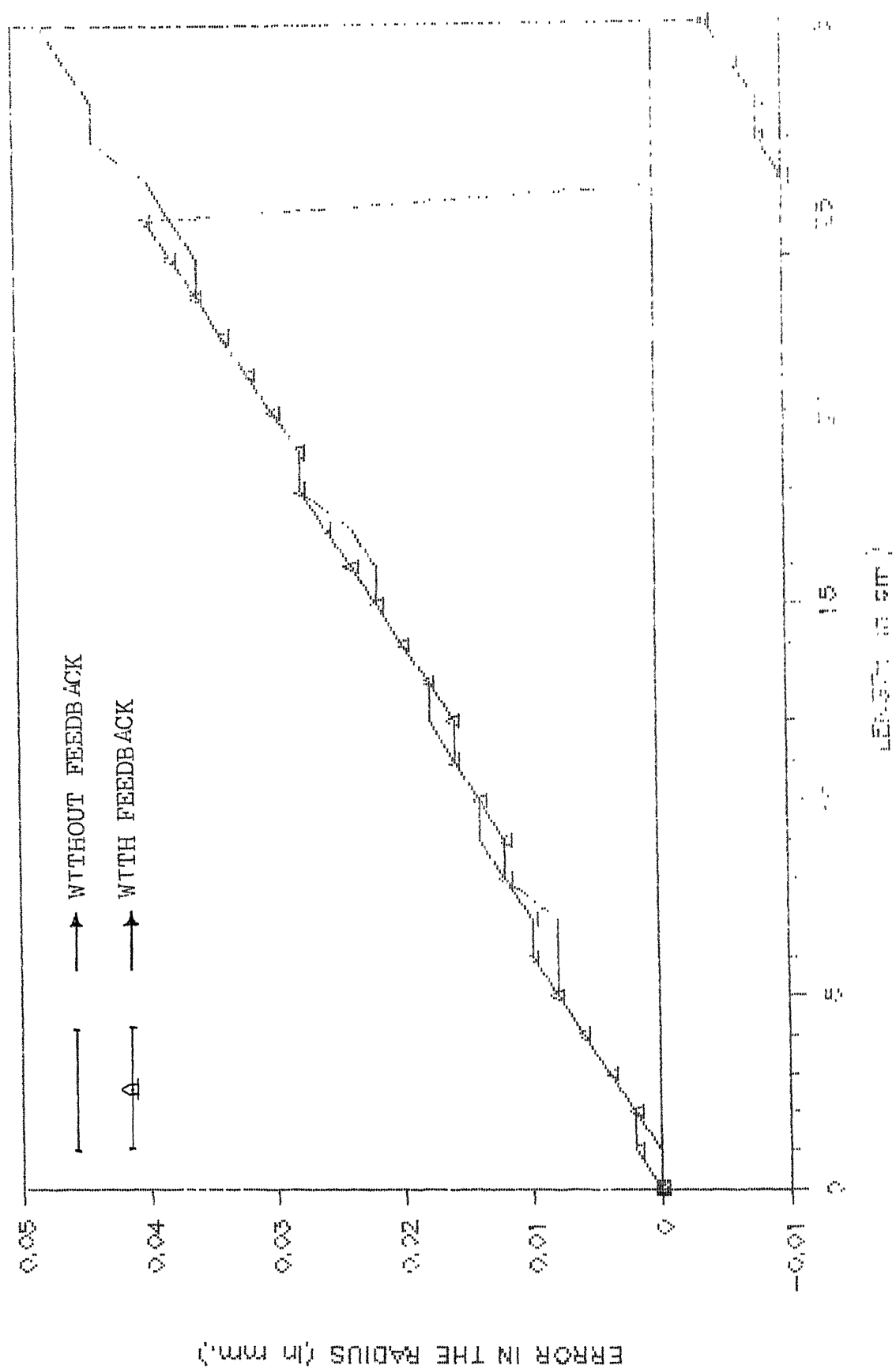


Fig. 4.9 Graph showing results of experiment -9

EXPERIMENT -9

Rotational Speed = 640 rpm  
 Feed = 0.05 mm/rev.  
 Original diameter = 28.58 mm  
 Desired diameter = 27.62 mm.  
 Cutting Speed = 57 m/min.

TABLE -9

Results of experiment -9

Sr. No.	Position along the length of cut cm.	Error in the radius with feedback mm.	Error in the Radius without feedback mm.
1	0.0	0.0	0.0
2	1.0	0.002	0.000
3	2.0	0.002	0.002
4	3.0	0.004	0.004
5	4.0	0.006	0.006
6	5.0	0.008	0.008
7	6.0	0.01	0.008
8	7.0	0.01	0.008
9	8.0	0.012	0.012
10	9.0	0.012	0.014
11	10.0	0.014	0.014
12	11.0	0.016	0.016
13	12.0	0.016	0.018
14	13.0	0.018	0.018
15	14.0	0.02	0.02
16	15.0	0.022	0.022
17	16.0	0.024	0.022
18	17.0	0.026	0.024
19	18.0	0.028	0.028
20	19.0	0.028	0.028
21	20.0	0.03	0.03
22	21.0	0.032	0.032
23	22.0	0.034	0.034
24	23.0	0.036	0.036
25	24.0	0.038	0.036
26	25.0	0.04	0.038
27	26.0	-0.01	0.04
28	27.0	-0.008	0.044
29	28.0	-0.008	0.044
30	29.0	-0.006	0.046
31	30.0	-0.004	0.048



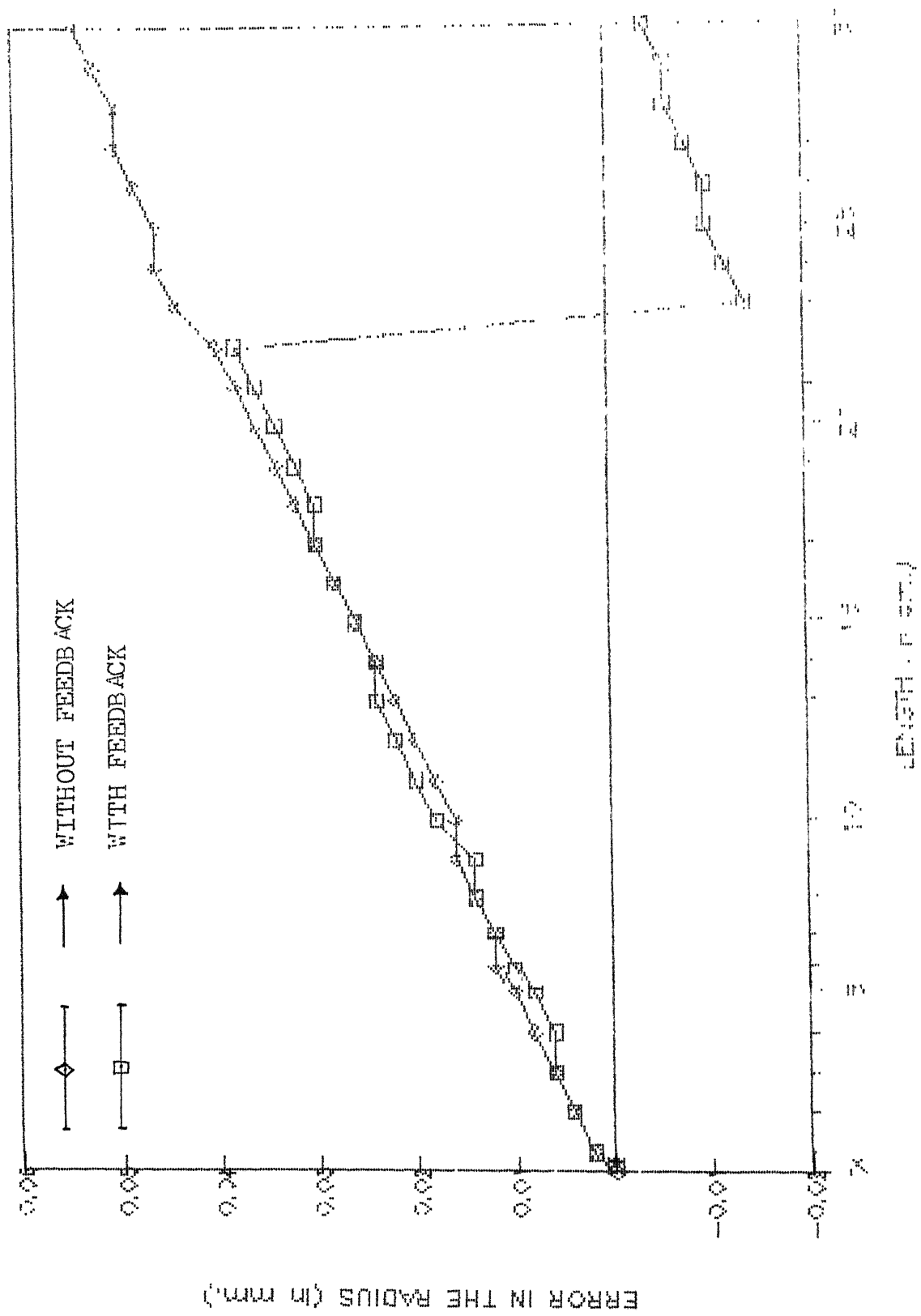


Fig. 4.10 Graph showing results of experiment -10

EXPERIMENT -10

Rotational Speed = 640 rpm

Feed = 0.063 mm/rev.

Original diameter = 27.62 mm

Desired diameter = 26.60 mm

Cutting Speed = 55 m/min

TABLE -10

Results of experiment -10

Sr. No.	Position along the length of cut cm.	Error in the radius with feedback mm.	Error in the Radius without feedback mm.
1	0.0	0.0	0.0
2	1.0	0.002	0.002
3	2.0	0.004	0.004
4	3.0	0.006	0.006
5	4.0	0.006	0.008
6	5.0	0.008	0.01
7	6.0	0.01	0.012
8	7.0	0.012	0.012
9	8.0	0.014	0.014
10.	9.0	0.014	0.016
11	10.0	0.018	0.016
12	11.0	0.02	0.018
13	12.0	0.022	0.02
14	13.0	0.024	0.022
15	14.0	0.024	0.024
16	15.0	0.026	0.026
17	16.0	0.028	0.028
18	17.0	0.03	0.03
19	18.0	0.03	0.032
20	19.0	0.032	0.034
21	20.0	0.034	0.036
22	21.0	0.036	0.038
23	22.0	0.038	0.04
24	23.0	-0.014	0.044
25	24.0	-0.012	0.046
26	25.0	-0.01	0.046
27	26.0	-0.01	0.048
28	27.0	-0.008	0.05
29	28.0	-0.006	0.05
30	29.0	-0.006	0.052
31	30.0	-0.004	0.054

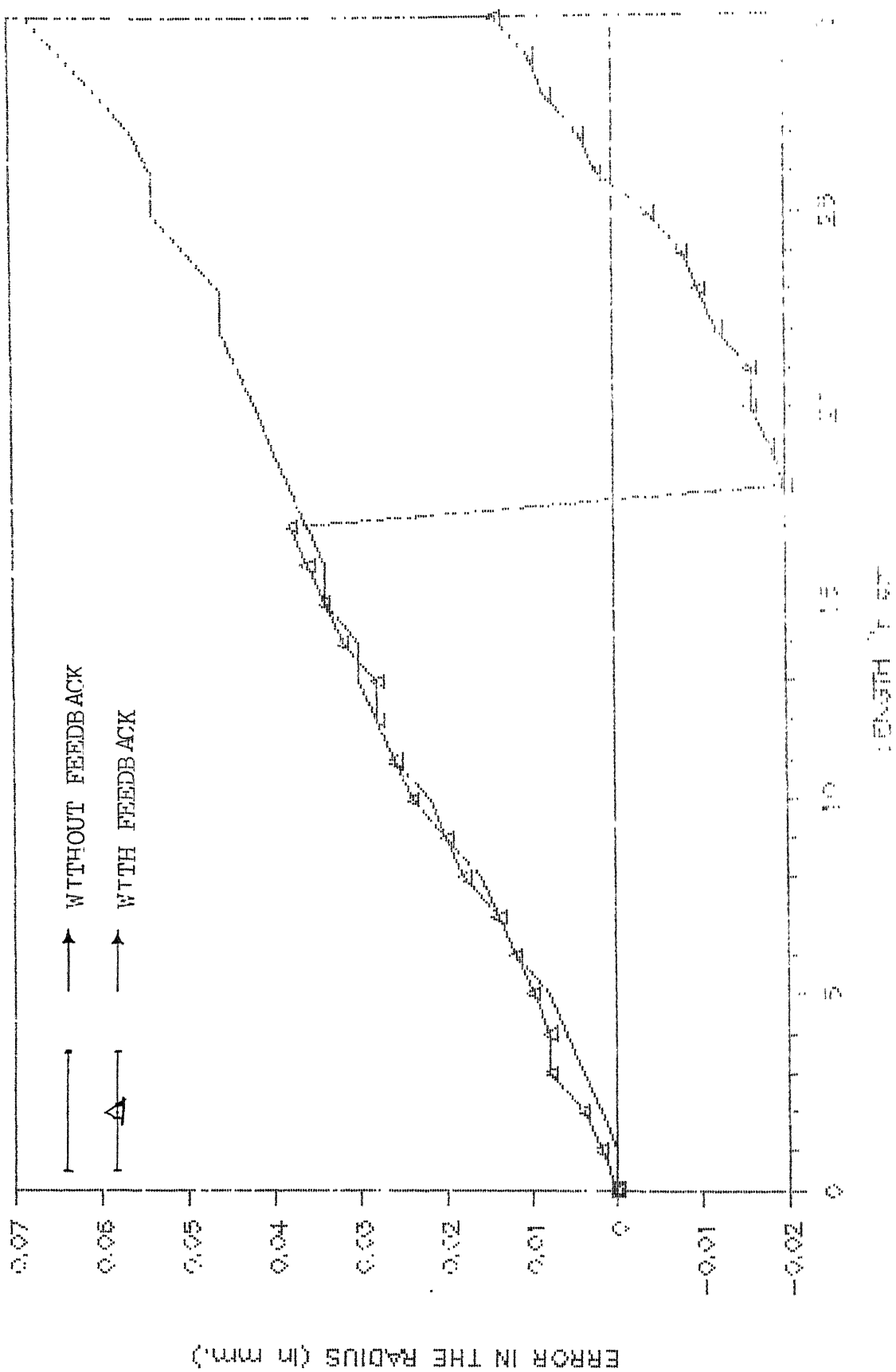


Fig. 4.11 graph showing results of experiment -11

EXPERIMENT -11

Rotational Speed = 640 rpm  
 Feed = 0.081 mm/rev.  
 Original diameter = 26.60 mm  
 Desired diameter = 25.56 mm  
 Cutting Speed = 52 m/min.

TABLE -11

Results of experiment -11

Sr. No.	Position along the length of cut cm	Error in the radius with feedback mm.	Error in the Radius without feedback mm.
1	0.0	0.0	0.0
2	1.0	0.002	0.000
3	2.0	0.004	0.002
4	3.0	0.008	0.004
5	4.0	0.008	0.006
6	5.0	0.01	0.008
7	6.0	0.012	0.012
8	7.0	0.014	0.014
9	8.0	0.018	0.016
10	9.0	0.02	0.02
11	10.0	0.024	0.022
12	11.0	0.026	0.026
13	12.0	0.028	0.028
14	13.0	0.028	0.03
15	14.0	0.032	0.03
16	15.0	0.034	0.034
17	16.0	0.036	0.034
18	17.0	0.038	0.036
19	18.0	-0.02	0.038
20	19.0	-0.018	0.04
21	20.0	-0.016	0.042
22	21.0	-0.016	0.044
23	22.0	-0.012	0.046
24	23.0	-0.01	0.046
25	24.0	-0.008	0.05
26	25.0	-0.004	0.054
27	26.0	0.002	0.054
28	27.0	0.004	0.056
29	28.0	0.008	0.060
30	29.0	0.01	0.064
31	30.0	0.014	0.068

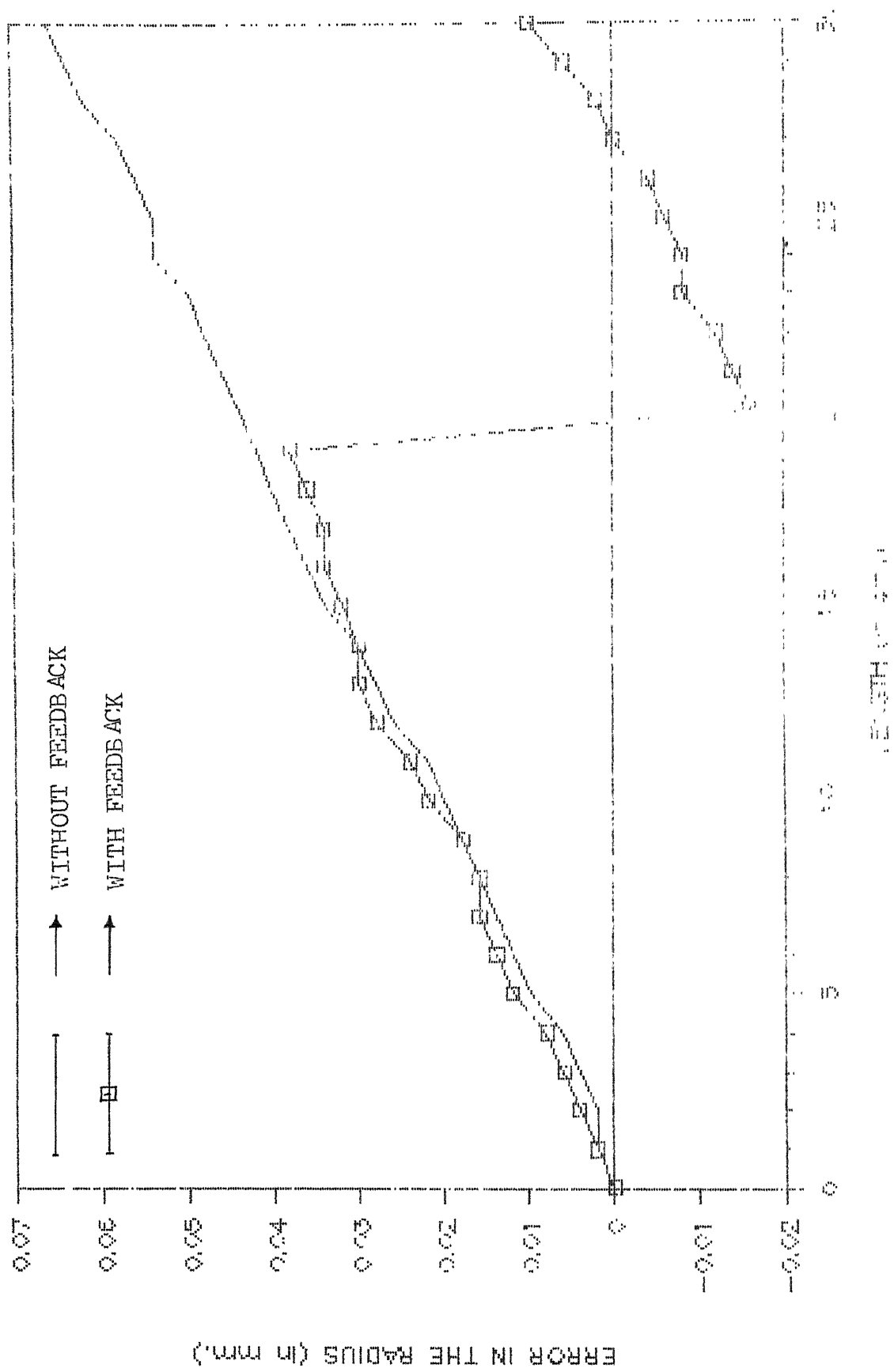


Fig. 4.12 Graph showing results of experiment -12

EXPERIMENT -12

Rotational Speed = 640 rpm.

Feed = 0.1 mm/rev.

Original diameter = 25.56 mm

Desired diameter = 24.62 mm

Cutting Speed = 50 m/min.

TABLE -12

Results of experiment -12

Sr. No.	Position along the length of cut cm	Error in the radius with feedback mm.	Error in the Radius without feedback mm.
1	0.0	0.0	0.0
2	1.0	0.002	0.002
3	2.0	0.004	0.002
4	3.0	0.006	0.004
5	4.0	0.008	0.006
6	5.0	0.012	0.01
7	6.0	0.014	0.012
8	7.0	0.016	0.014
9	8.0	0.016	0.016
10	9.0	0.018	0.018
11	10.0	0.022	0.02
12	11.0	0.024	0.022
13	12.0	0.028	0.026
14	13.0	0.03	0.028
15	14.0	0.03	0.03
16	15.0	0.032	0.034
17	16.0	0.034	0.036
18	17.0	0.034	0.038
19	18.0	0.036	0.04
20	19.0	0.038	0.042
21	20.0	-0.016	0.044
22	21.0	-0.014	0.046
23	22.0	-0.012	0.048
24	23.0	-0.008	0.05
25	24.0	-0.008	0.054
26	25.0	-0.006	0.054
27	26.0	-0.004	0.056
28	27.0	0.000	0.058
29	28.0	0.002	0.062
30	29.0	0.006	0.064
31	30.0	0.01	0.066

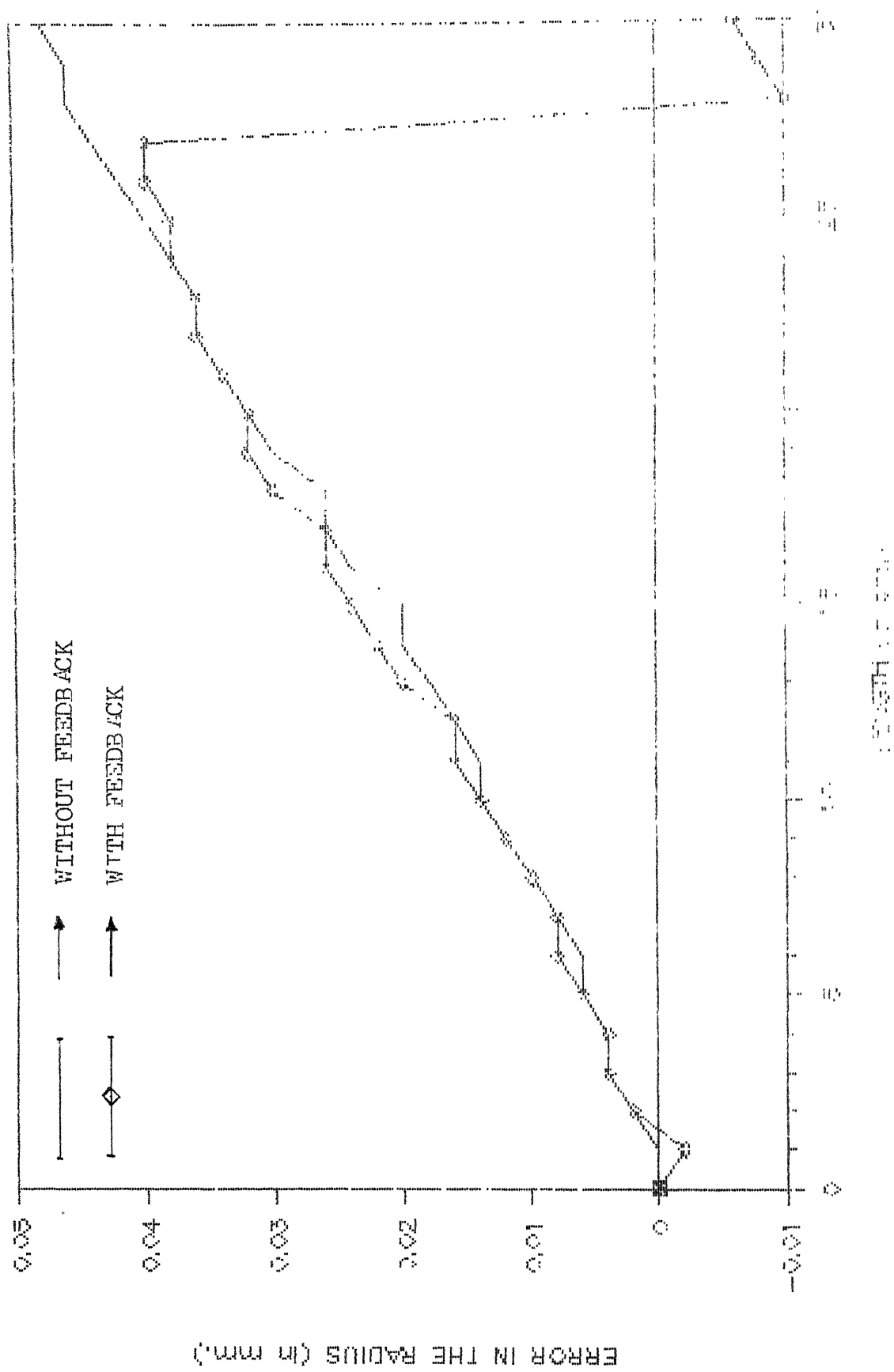


Fig. 4.13 graph showing results of experiment -13

EXPERIMENT -13

Rotational Speed = 500 rpm  
 Feed = 0.05 mm/rev.  
 Original diameter = 24.62 mm  
 Desired diameter = 23.60 mm  
 Cutting speed = 38 m/min.

TABLE -13

Results of experiment -13

Dr. No.	Position along the length of cut cm.	Error in the radius with feedback mm.	Error in the Radius without feedback mm.
1	0.0	0.0	0.0
2	1.0	-0.002	0.000
3	2.0	0.002	0.002
4	3.0	0.004	0.004
5	4.0	0.004	0.004
6	5.0	0.006	0.006
7	6.0	0.008	0.006
8	7.0	0.008	0.008
9	8.0	0.01	0.01
10	9.0	0.012	0.012
11	10.0	0.014	0.014
12	11.0	0.016	0.014
13	12.0	0.016	0.016
14	13.0	0.02	0.018
15	14.0	0.022	0.02
16	15.0	0.024	0.02
17	16.0	0.026	0.024
18	17.0	0.026	0.026
19	18.0	0.03	0.026
20	19.0	0.032	0.03
21	20.0	0.032	0.032
22	21.0	0.034	0.034
23	22.0	0.036	0.036
24	23.0	0.036	0.036
25	24.0	0.038	0.038
26	25.0	0.038	0.04
27	26.0	0.04	0.042
28	27.0	0.04	0.044
29	28.0	-0.01	0.046
30	29.0	-0.008	0.046
31	30.0	-0.006	0.048



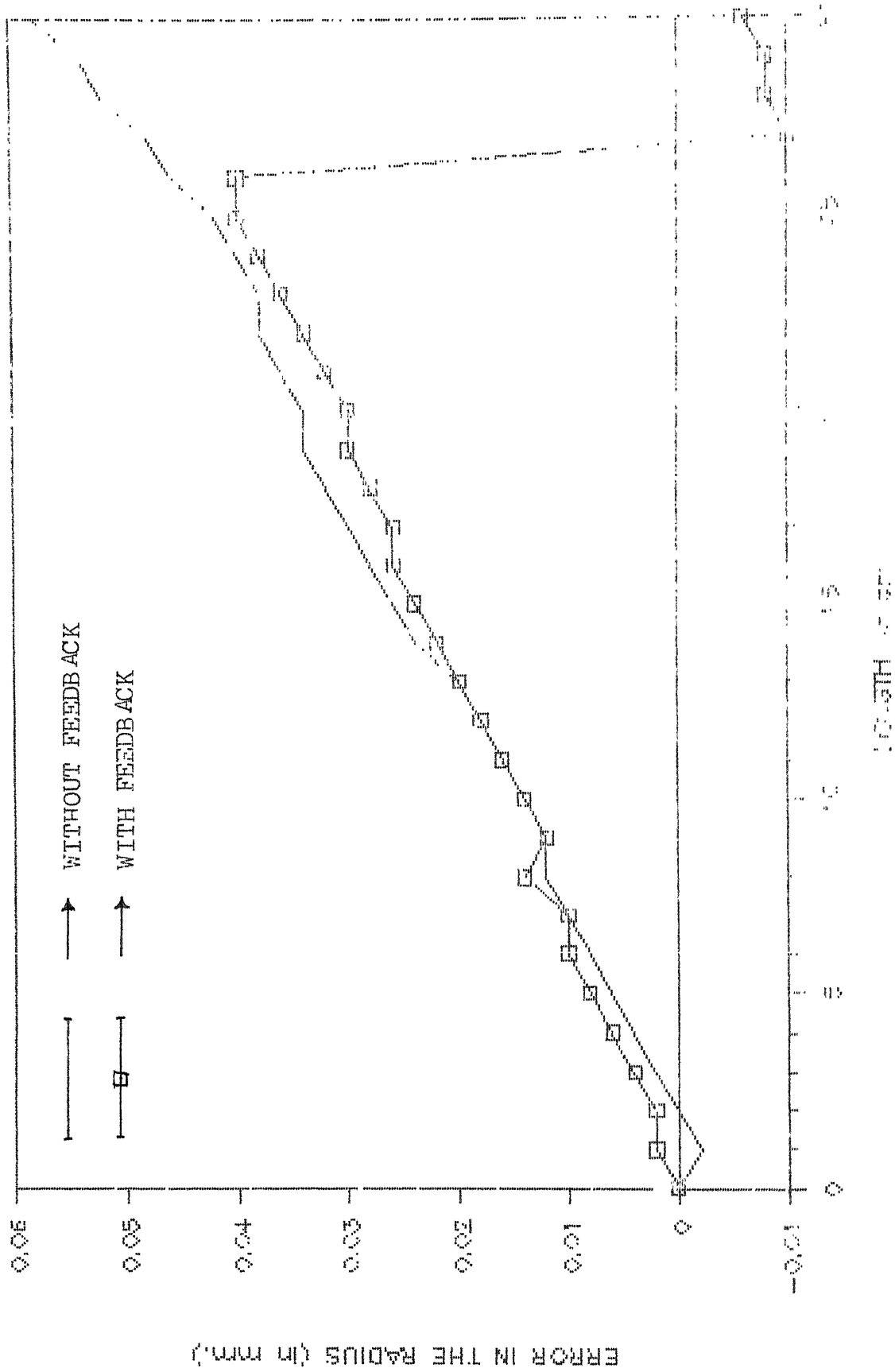


Fig. 4.14 Graph showing results of experiment -14

EXPERIMENT -14

Rotational Speed = 500 rpm  
 Feed = 0.063 mm/rev.  
 Original diameter = 23.60 mm  
 Desired diameter = 22.56 mm  
 Cutting Speed = 36 m/min.

TABLE -14

Results of experiment -14

Sr. No.	Position along the length of cut cm.	Error in the radius with feedback mm.	Error in the Radius without feedback mm.
1	0.0	0.0	0.0
2	1.0	0.002	-0.002
3	2.0	0.002	0.000
4	3.0	0.004	0.002
5	4.0	0.006	0.004
6	5.0	0.008	0.006
7	6.0	0.01	0.008
8	7.0	0.01	0.01
9	8.0	0.014	0.012
10	9.0	0.012	0.012
11	10.0	0.014	0.014
12	11.0	0.016	0.016
13	12.0	0.018	0.018
14	13.0	0.02	0.02
15	14.0	0.022	0.024
16	15.0	0.024	0.026
17	16.0	0.026	0.028
18	17.0	0.026	0.03
19	18.0	0.028	0.032
20	19.0	0.03	0.034
21	20.0	0.03	0.034
22	21.0	0.032	0.036
23	22.0	0.034	0.038
24	23.0	0.036	0.038
25	24.0	0.038	0.04
26	25.0	0.04	0.042
27	26.0	0.04	0.046
28	27.0	-0.01	0.048
29	28.0	-0.008	0.052
30	29.0	-0.008	0.054
31	30.0	-0.006	0.058

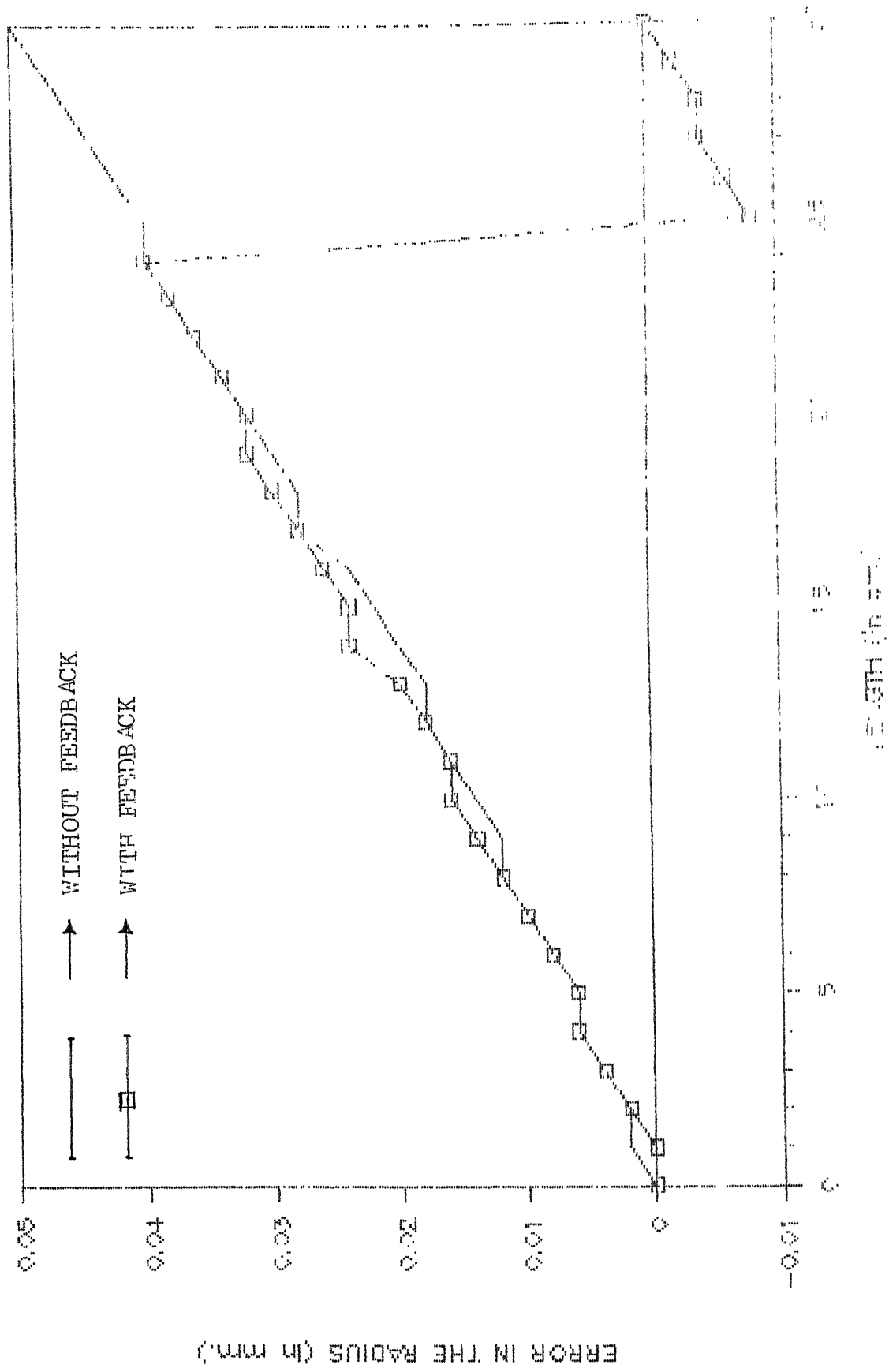


Fig. 4.15 Graph showing results of experiment -15

EXPERIMENT -15

Rotational Speed = 500 rpm  
 Feed = 0.081 mm/rev.  
 Original diameter = 22.56 mm  
 Desired diameter = 21.58 mm  
 Cutting Speed = 35 m/min.

TABLE -15

Results of experiment -15

Dr. No.	Position along the length of cut cm.	Error in the radius with feedback mm.	Error in the Radius without feedback mm.
1	0.0	0.0	0.0
2	1.0	0.0	0.002
3	2.0	0.002	0.002
4	3.0	0.004	0.004
5	4.0	0.006	0.006
6	5.0	0.006	0.006
7	6.0	0.008	0.008
8	7.0	0.01	0.01
9	8.0	0.012	0.012
10	9.0	0.014	0.012
11	10.0	0.016	0.014
12	11.0	0.016	0.016
13	12.0	0.018	0.018
14	13.0	0.02	0.018
15	14.0	0.024	0.02
16	15.0	0.024	0.022
17	16.0	0.026	0.024
18	17.0	0.028	0.028
19	18.0	0.03	0.028
20	19.0	0.032	0.03
21	20.0	0.032	0.032
22	21.0	0.034	0.034
23	22.0	0.036	0.036
24	23.0	0.038	0.038
25	24.0	0.04	0.04
26	25.0	-0.008	0.04
27	26.0	-0.006	0.042
28	27.0	-0.004	0.044
29	28.0	-0.004	0.046
30	29.0	-0.002	0.048
31	30.0	0.0	0.05

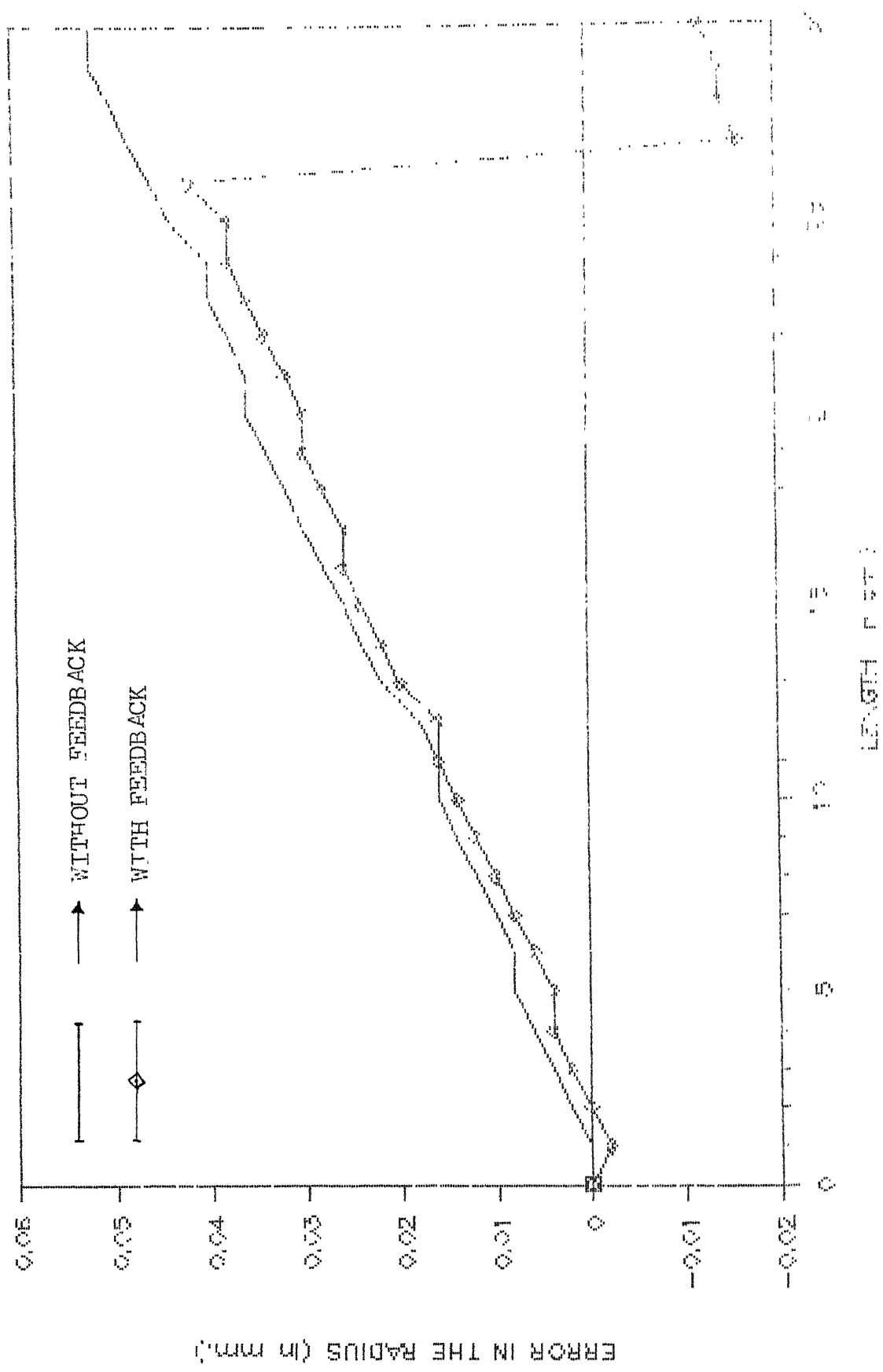


Fig. 4.16 Graph showing results of experiment -16

EXPERIMENT -16

Rotational Speed = 500 rpm  
 Feed = 0.081 mm/rev.  
 Original diameter = 21.58 mm  
 Desired diameter = 20.60 mm  
 Cutting Speed = 33 m/min.

TABLE -16

Results of experiment -16

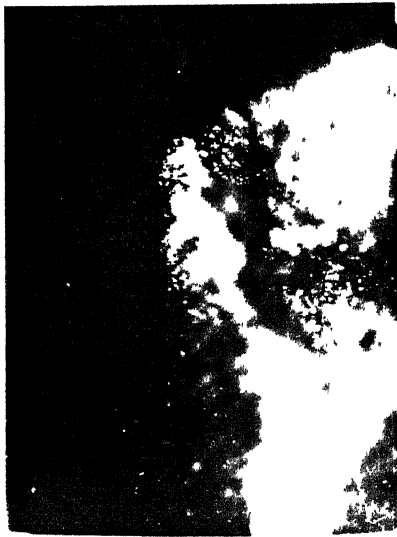
Dr. No.	Position along the length of cut cm.	Error in the radius with feedback mm.	Error in the Radius without feedback mm.
1	0.0	0.0	0.0
2	1.0	-0.002	0.0
3	2.0	0.0	0.002
4	3.0	0.002	0.004
5	4.0	0.004	0.006
6	5.0	0.004	0.008
7	6.0	0.006	0.008
8	7.0	0.008	0.01
9	8.0	0.01	0.012
10	9.0	0.012	0.014
11	10.0	0.014	0.016
12	11.0	0.016	0.016
13	12.0	0.016	0.018
14	13.0	0.02	0.022
15	14.0	0.022	0.024
16	15.0	0.024	0.026
17	16.0	0.026	0.028
18	17.0	0.026	0.03
19	18.0	0.028	0.032
20	19.0	0.03	0.034
21	20.0	0.03	0.036
22	21.0	0.032	0.036
23	22.0	0.034	0.038
24	23.0	0.036	0.04
25	24.0	0.038	0.04
26	25.0	0.038	0.044
27	26.0	0.042	0.046
28	27.0	-0.016	0.048
29	28.0	-0.014	0.05
30	29.0	-0.014	0.052
31	30.0	-0.012	0.052

TABLE -17

Co-efficients of error reduction for  
same feed but different speeds.

sr. no.	Experiment Nos.	Cutting speed m/min.	Feed mm/rev.	Co-efficient of error reduction E
1	1	114	0.05	0.5448
2	5	81	0.05	0.3793
3	9	57	0.05	0.1667
4	13	38	0.05	0.1667
5	2	111	0.063	0.5909
6	6	78	0.063	0.4545
7	10	55	0.063	0.2963
8	14	36	0.063	0.3003
9	3	108	0.081	0.5135
10	7	76	0.081	0.2692
11	11	52	0.081	0.4412
12	15	35	0.081	0.2000
13	4	104	0.1	0.6538
14	8	73	0.1	0.5384
15	12	50	0.1	0.4242
16	16	33	0.1	0.1923

TOOL -1



TOOL -2



TOOL -3



TOOL -4

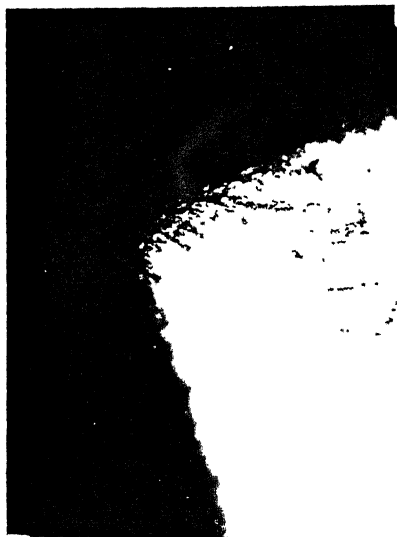


Fig. 4.17

TOOL 1, 2, 3 and 4



TOOL -5



TOOL -6



TOOL -7



TOOL -8



Fig. 4.18

TOOL 5,6,7 and 8

TOOL -9



TOOL -10



TOOL -11



TOOL -12

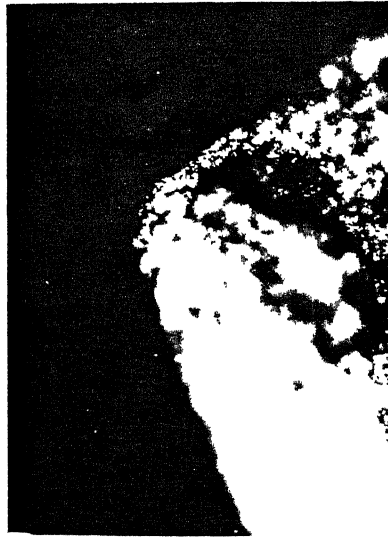


Fig. 4.19 TOOL 9,10,11 and 12

TOOL -13



TOOL -14



TOOL -15



TOOL -16



Fig. 4.20 TOOL 13,14,15 and 16

#### 4.2 DISCUSSION :

From the results tabulated and plotted on the graph it can be seen that the error has been reduced to some extent in all the experiments when the feedback control had been used. Feedback control causes reduction in the error which is proportional to the toolwear. The co-efficient of error reduction should increase with the toolwear and hence with decrease in the speed the co-efficient of error reduction should decrease. This was found to be the case in most of the cases as can be seen from table 17.

In table 17 co-efficients of error reduction for the same feed but different cutting speeds are compared. It can be seen that the co-efficient of error reduction in experiment 13 with feed of 0.05 mm and speed of 38 m/min. is higher than what can be expected from the previous experiment with same feed. This means that more toolwear has taken place than expected. The reason for this can be inhomogeneity in the workpiece. Same is the case with experiment 14 and experiment 11 and for this also inhomogeneity in the workpiece can be the reason. Apart from this the toolwear and hence the coefficient of error reduction decreases with the decrease in the speed for the same feed.

From tables 1 to 16 it is seen that the sensitivity of the system increases with increase in curvature of the workpiece because the assumption that the workpiece is flat fails with reduction in work diameter. The sensitivity is 0.036 mm when work diameter is 35.76 mm which deteriorates to 0.042 mm when work diameter is 21.58 mm.

#### 4.3 CONCLUSIONS :

An online control system has been designed and tested experimentally. The main objective of improving dimensional stability by compensating the toolwear has been fulfilled. The error in the radius has been restricted to 0.042 mm in the worst case and 0.034 mm in the best. The performance of the control system was tested for a range of cutting conditions and the system was found to work effectively. However, with increase in the curvature the system becomes less effective because of the abovementioned reason.

The following objectives have been fulfilled.

- i) Design and fabrication of a sensing device to sense toolwear during machining.
- ii) Selection of an actuator to position the toolpost according to the tool wear.
- iii) Design and fabrication of a feedback control system components that connect the sensing and compensating components.
- iv) Assembly and testing of the system designed and fabricated.

#### 4.4 SCOPE FOR FUTURE WORK :

The present work can be extended further. The system sensitivity can be improved by using smaller orifice and nozzle. By using a pilot-controlled direction control valve having smaller operating pressure range the sensitivity can be improved.

Apart from this hydraulic power can be used for tool actuation to give faster response. The performance of the system can be greatly improved if the compensation is carried out in steps rather than in a single stroke. For this pneumatic signal available from the sensor should be converted in the electric pulses and pulses should be given to the electro-hydraulic stepper motor which would act as an actuator. This system is likely to give the accuracy of the order of 0.001 mm.

REFERENCES

1. M.E. Merchant, H. Ernst and E.J. Krabacher, "Radioactive cutting tools for rapid tool-life Testing", Trans. ASME, May 1953.
2. N.H. Cook, K. Subramaniam and Merchant "Micro-Isotope toolwear sensor " ,Annals of the CIRP, Vol. 27, 1978.
3. Slavko M. Arsovski, "Wear sensors in the adaptive control systems of machine tools", Int. Jour. of Production Research, vol. 21, No.3, 1983.
4. A.J. Wilkinson, "Constriction resistance concept applied to wear measurement of metal cutting tools", Proceedings of IEE 1971, vol. 118, No.2.
5. S. Jetly, "Measuring toolwear on-line : Some practical considerations" Manufacturing Engineering, July 1984.
6. E.J. Weller, H.M. Schrier and B. Weichbrodt, "What sound can be expected from a worn tool ?", Jour. of Engineering for Industry, Trans. ASME, August 1969.
7. E. Emel and E. Kannatey, "Tool failure monitoring in turning by pattern recognition analysis of AE signals", Jour. of Engineering for Industry. Trans. ASME May 1988, vol. 110.
8. L.V. Colwell, "Tracking tool deterioration by computer", Annals of CIRP, 1974, vol. 23/1.

9. K. Uehara, "Automatic toolwear monitoring in NC turning", Annals of CIRP, 1979, vol. 28/1.
10. H. Suzuki and K.J. Weinmann, "An online toolwear sensor for straight turning operations", Jour. of Engineering for Industry, Trans. ASME, November 1985, vol. 107.
11. J.I. El Gomayel and K.D. Bregger, "Online toolwear sensing for turning operations", Jour. of Engineering for Industry, Trans. ASME, February 1986, vol. 108.
12. Y. Maeda, H. Uchida and A Yamamoto, "Estimation of wear land width of cutting tool flank with the aid of digital image processing technique ", Bull. Japan Society of precesion Engineering September 1987, vol. 21.
13. M. Shiraishi and K. Uehara, "In-process control of workpiece dimension in turning", Annals of CIRP, 1979, vol. 28/1.
14. C.W. Park, K.F. Eman and S.M. Wu, "An in-process flatness error measurement and compensatory control system", Jour. of Engineering for Industry, Trans. ASME, August 1988, vol. 110.
15. R.K. Jain  
Engineering Metrology.



APPENDIX -1CUTTING TOOL GEOMETRY

Back rake angle	-	0°
Side rake angle	-	12°
End cutting edge angle	-	8°
Side cutting edge angle	-	5°
End relief angle	-	8°
Side relief angle	-	8°
Nose radius	-	0.0
Tool size	-	1/2"

APPENDIX -2THE MACHINE TOOL

Type : HMT LB17 Centre lathe

Centre height : 170 mm.

Centre distance : 1000 mm.

Swing over bed : 350 mm.

Swing over cross  
slide : 170 mm.

Motor : 10 HP/3000 rpm

Spindle speed : 18, 45 to 2000 rpm.